Hindawi
Journal of Mathematics
Volume 2021, Article ID 6683083, 28 pages
https://doi.org/10.1155/2021/6683083

Research Article

Theoretical Derivation and Parameters Analysis of a Human-Structure Interaction System with the Bipedal Walking Model

Huiqi Liang[1,2], **Zhiqiang Zhang**[1,2] **and Peizi Wei**[1,2]

[1]*Key Laboratory of Concrete and Prestressed Concrete Structure, Ministry of Education, Southeast University, Nanjing 210096, China*
[2]*School of Civil Engineering, Southeast University, Nanjing 210096, China*

Correspondence should be addressed to Zhiqiang Zhang; 230208105@seu.edu.cn

Received 13 December 2020; Revised 14 January 2021; Accepted 30 January 2021; Published 3 March 2021

Academic Editor: Imtiaz Ahmad

The excessive vertical vibration of structures induced by walking pedestrians has attracted considerable attention in the past decades. The bipedal walking models proposed previously, however, merely focus on the effects generated by legs and ignore the effects of the dynamics of body parts on pedestrian-structure interactions. The contribution of this paper is proposing a novel pedestrian-structure interaction system by introducing the concept of the continuum and a different variable stiffness strategy. The dynamic model of pedestrian-structure coupling system is established using the Lagrange method. The classical mode superposition method is utilized to calculate the response of the structure. The state-space method is employed to determine natural frequencies and damping ratio of the coupled system. Based on the proposed model, numerical simulations and parametric analysis are conducted. Numerical simulations have shown that the continuum enables the pedestrian-structure system to achieve the stable state more efficiently than the classic model does, which idealizes the body as a concentrated or lumped mass. The parametric study reveals that the presence of pedestrians is proved to significantly decrease the frequency of human-structure interaction system and improve its damping ratio. Moreover, the parameters of the bipedal model have a noticeable influence on the dynamic properties and response of the pedestrian-structure system. The bipedal walking model proposed in this paper depicts a pattern of pedestrian-structure interactions with different parameter settings and has a great potential for a wide range of practical applications.

1. Introduction

In recent years, the problem of human-induced vibration in flexible bridges has attracted extensive attention, which makes the improvement of bridge vibration serviceability a necessary consideration in new structure design [1]. To meet the architectural requirement of aesthetics, footbridges that only bear pedestrian loads tend to exhibit long, light, flexible, and fewer degrees of freedom, which makes footbridges more sensitive to human-induced vibration.

To assess the vibration serviceability of new footbridges, the moving force (MF) model is generally adopted by many guidelines (e.g., OHBDC [2], BS 5400 [3], ISO-10137 [4], Eurocode 5 [5], Setra [6], and HIVOSS [7]). However, this approach does not consider the impact of pedestrians on the properties of the structural system (such as frequency and damping), nor does it consider the impact of structural vibrations upon pedestrian gait, as excessive vibrations would produce panic among pedestrians [8–10]. Later, new human-structure models are updated to simulate the interactions between humans and structure to further evaluate pedestrian-induced structural responses. To explore the contribution of the pedestrian mass to the structure, Biggs [11] simulates the human body as a moving mass, which fully accounts for the mass coupling between the human body and the structure, known as the MM (moving mass) model. Although the MM model can interpret the effect of the crowd on the frequency of the structure, it fails to explain

the additional damping of the structure induced by the crowd, and the dynamic behaviours of the crowd-structure system are quite distinct from those of the unloaded structure [12–14]. Several studies have shown that pedestrians provide negligible additional damping to structures subjected to vertical vibration [14–17]. Therefore, to depict the dynamic behaviour of the human body, some researchers have equated pedestrians to SMD system, which accounts for the effects of human mass, stiffness, and damping on the structure [18–22]. The moving SMD, introduced by Archbold [18], is applied into the HSI area and the SMD model has a better predictability in vibration response as compared to the MF model [20]. Although the SMD model considers the dynamic properties of the human body and replaces GRF with a predefined mobility force with double-peak characteristics, it ignores the gait characteristics of the human body with switching legs in the walking process.

In the field of biomechanics, the inverted pendulum model is commonly applied to the study of human gait and GRF. The bipedal walking model yields a GRF with a twin peaks feature, which agrees well with the experimental data, suggesting that the bipedal inverted pendulum model can represent the kinetics of human walking well [23–26]. Qin et al. [27, 28] present a viable solution to the problem of human-structure interaction based on a biomimetic bipedal walking model and address the model's instability in gait continuity due to damping energy dissipation by imposing a control force. However, the limitation of Qin's model is evident for it is dynamically unstable when applied to the crowds due to the strict energy compensation mechanism, which results in the model's vulnerability to initial conditions. To extend the bipedal model to the interaction between the crowds and the structure, Gao et al. [29] develop a self-determining walking velocity mechanism to enhance the gait stability, which has been implemented to define crowd-structure interaction [30]. Yang and Gao [31] recommend a similar pedestrian-structure system to explore the impact of humans on structural dynamic properties based on a bipedal walking model.

However, the bipedal walking models mentioned above all assume that the mass of the body is concentrated in the center of gravity, due to which the model only involves the impact of stiffness and damping of the legs but ignores the dynamics of other parts of the body. Although this approach may simplify the model, it ignores the dynamic properties of the human body which vary along the height of the body and fails to examine its influence on the whole system. To overcome the limitation of models that concentrate on the mass of the body, we have equated other human body parts except the legs to a continuum for the first time when the interaction between the human and the structure is considered. It is shown that the existence of the continuum allows the human-structure system to be stabilized more efficiently. Moreover, the results show that the damping of the continuum would influence the response of the coupled system, which has not been reported in previous research. It reveals a necessity to consider the effect of the continuum if the interaction between human and structure is calculated. A different leg stiffness strategy that involves more parameters is taken to simulate the dynamic properties of the legs in a more comprehensive way. It is found that the stiffness strategy we proposed reveals more features of the GRF in shape and peak value.

As regards the contribution of this study, it is an extension of the works of Gao et al. [29] and Qin et al. [27, 28] in that we innovatively substitute the concentrated mass of the bipedal walking model with a continuum body and the corresponding dynamic equations are derived from the Lagrangian equation. This approach provides a solution to examine the effect of the distribution of stiffness, mass, and damping of other body parts on the structural response and dynamic properties. Moreover, it allows the system to reach a stable state more efficiently if compared to the classical model. Another distinctive feature of the proposed model is its adoption of time-dependent leg stiffness, which includes the loss of stiffness as one's foot leaves the ground and is different from the strategy adopted by others. This allows for the exploration of more leg parameters of the coupled system.

The outline of the paper is as follows. Section 2 presents the theoretical formulae of vertical vibration based on a walking bipedal pedestrian-structure model that considers human mass, stiffness, and damping distribution as impact factors in pedestrian-structure interaction. Part 3 presents an overview of how to obtain real-time dynamic properties of a pedestrian-structure interaction system by solving the spatial equations of state. The calculation procedure of the pedestrian-structure model is given in Section 4. Part 5 explores the effect of a pedestrian on the structure with a realistic numerical example, the result of which is also compared with Gao's. In Section 6, the effect of the dynamic parameters of a bipedal walking model on the structural response and dynamic performance is detailly analyzed. Simulation results of various parameters of the model are discussed in Section 7. Section 8 summarizes the paper.

2. Pedestrian-Structure Dynamic Interaction System

2.1. Introduction of the Bipedal Walking Model. The model of pedestrian-structure interaction can be represented by a bipedal inverted pendulum model with a simple Euler–Bernoulli beam with span length Lb. To quantify the dynamics of the human body, the body can be modelled as a continuous bar with mass distribution $m(x)$, damping distribution $c(x)$, and stiffness distribution $k(x)$. Although $m(x)$, $c(x)$, and $k(x)$ are unknown at present, we denote the arbitrary distribution by the three parameters. The vertical motion of a body relative to a fixed base can be described by means of the mode superposition method, where $z_{\mathrm{HR}}(u,t)$ is the body motion relative to the stationary base upon which the body stands. In the model, the stationary base denotes the intersection of the two legs, representing the lowest point of the continuum. For the convenience of derivation, only the first two modes of the continuum are presented in the paper. $\phi_{\mathrm{HR1}}(u)$ and $\phi_{\mathrm{HR2}}(u)$ are the shapes of the first and the second mode of vertical vibration along the standing body. $z_{\mathrm{HR1}}(t)$ and $z_{\mathrm{HR2}}(t)$ refer to the generalized modal

coordinates of the first and the second mode relative to the fixed base and can be expressed as follows:

$$z_{\mathrm{HR}}(u,t) = z_{\mathrm{HR1}}(t)\phi_{\mathrm{HR1}}(u) + z_{\mathrm{HR2}}(t)\phi_{\mathrm{HR2}}(u) + \cdots, \tag{1a}$$

$$\dot{z}_{\mathrm{HR}}(u,t) = \dot{z}_{\mathrm{HR1}}(t)\phi_{\mathrm{HR1}}(u) + \dot{z}_{\mathrm{HR2}}(t)\phi_{\mathrm{HR2}}(u) + \cdots, \tag{1b}$$

where $x_l(t)$ and $x_t(t)$, respectively, denote the coordinates along the x-direction of the contact points of the pedestrian's leading and trailing legs with the Euler–Bernoulli beam. $w(x_l,t)$ and $w(x_t,t)$, respectively, represent the displacement of the beam at x_l and $x_t$from the system's equilibrium position in the vertical direction. The distance between the intersection of the legs and the horizontal axis is denoted by $z_H(t)$, and this intersection point is the base of the continuum. $x_{\mathrm{HR}}(t)$ indicates the horizontal coordinates of the intersection of the legs, m_{HR} signifies the total mass of the continuum, and $k_{\mathrm{HR}}(u)$ denotes the stiffness distribution of the body. $k_l(t)$ and $c_l(t)$ denote the stiffness and damping of the leading leg, respectively. $k_t(t)$ and $c_t(t)$ denote the stiffness and damping of the trailing leg, respectively. What merits special attention is that leg stiffness and damping, both functions of time, change along with the progression of human gait. For convenience of presentation, the model in Figure 1 represents a walking pedestrian in the crowd, and the interaction between the crowd and the structure is taken into account in the derivation of the formula.

2.2. Dynamic Equation of the Pedestrian-Structure System. We assume that at least one foot of the walking pedestrian is in contact with the structure, that is, without considering the case where both feet are not in touch with the structure. To improve the stability of the predicted gait, Gao and Yang [30] adopted a self-determined mechanism to determine the velocity of pedestrians; that is, the velocity of pedestrians is a given quantity. This approach addresses the instability of the walking model due to the dissipation of energy caused by leg damping and is fully compatible with the characteristics of the human walking process and can be adapted to a more complex walking condition. The vertical dynamic equation of pedestrian-structure system is derived from Lagrange equation [32]. The total kinetic energy $T$and potential energy V of the pedestrian-structure interaction system in the double-leg support can be obtained as follows:

$$\begin{aligned} V = {} & \frac{1}{2}\sum_{i=1}^{N}\left[\int_0^L k_{\mathrm{HR}_i}(u)\left(\frac{\partial z_{\mathrm{HR}_i}(u,t)}{\partial u}\right)^2 \mathrm{d}u + k_{li}\left(L_0 - L_l(t)\right)^2 + k_{ti}\left(L_0 - L_t(t)\right)^2\right] \\ & + \sum_{i=1}^{N}\int_0^H m_i(u)\left(z_{\mathrm{HR}_i}(u,t) + z_{Hi}(t)\right)g\,\mathrm{d}u + \frac{1}{2}\int_0^{Lb}\mathrm{EI}w''^2(x,t)\mathrm{d}x, \end{aligned} \tag{2a}$$

$$T = \sum_{i=1}^{N}\frac{1}{2}m_{\mathrm{HR}_i}\left(\dot{x}_{\mathrm{HR}_i}(t)^2\right) + \sum_{i=1}^{N}\frac{1}{2}\int_0^H m_i(u)\left(\dot{z}_{\mathrm{HR}_i}(u,t) + \dot{z}_{Hi}(t)\right)^2\mathrm{d}u + \frac{1}{2}\int_0^{Lb}\overline{m}\dot{w}^2(x,t)\mathrm{d}x, \tag{2b}$$

where L_0, a constant, denotes the initial length of the leg spring. $L_l(t)$ and $L_t(t)$ indicate the instantaneous length of the leading and trailing legs. $\dot{x}_{\mathrm{HR}_i}$ and $\dot{z}_{Hi}(t)$ represent the horizontal and vertical velocities of the continuum. $\overline{m}$ represents the mass of the beam per meter, and $\dot{z}_{\mathrm{HR}_i}(u,t)$ indicates the vertical velocity at a certain point of the continuum. $w'' = (\partial^2 w(x,t)/\partial x^2)$ and $\dot{w} = (\partial w(x,t)/\partial t)$ are curvature and vertical vibrational velocity of the beam, respectively. E is the modulus of elasticity of the material, I is the moment of inertia of the cross section of the beam, N denotes the number of pedestrians, and i refers to the ith person. To facilitate the derivation of the proposed algorithm, we will not use the subscript i to distinguish each pedestrian in the derivation below. Based on the empirical mode decomposition method, the displacement of a certain point on the beam can be obtained by superimposing the first several modes of vibration:

$$\begin{aligned} w(x,t) &= \Phi(x)Y(t) = \sum_{j=1}^{n}\phi_j(x)Y_j(t), \\ \dot{w}(x,t) &= \sum_{j=1}^{n}\phi_j(x)\dot{Y}_j(t), \end{aligned} \tag{3}$$

where $\phi_j(x)\{j = 1,2,\ldots,n\}$ is defined as the vibration mode, $Y_j(t)\{j = 1,2,\ldots,n\}$ is the generalized modal coordinates, $\dot{Y}_j(t) = \mathrm{d}Y_j(t)/\mathrm{d}t$ denotes the derivative of generalized coordinates over time, and n represents the mode number of the structure considered in the analysis.

The length of the leading and trailing legs of a given pedestrian can be denoted as

$$L_l(t) = \sqrt{\left(x_{\mathrm{HR}}(t) - x_l\right)^2 + \left(z_H(t) - w(x_l,t)\right)^2}, \tag{4a}$$

$$L_t(t) = \sqrt{\left(x_l(t) - x_t\right)^2 + \left(z_H(t) - w(x_t,t)\right)^2}. \tag{4b}$$

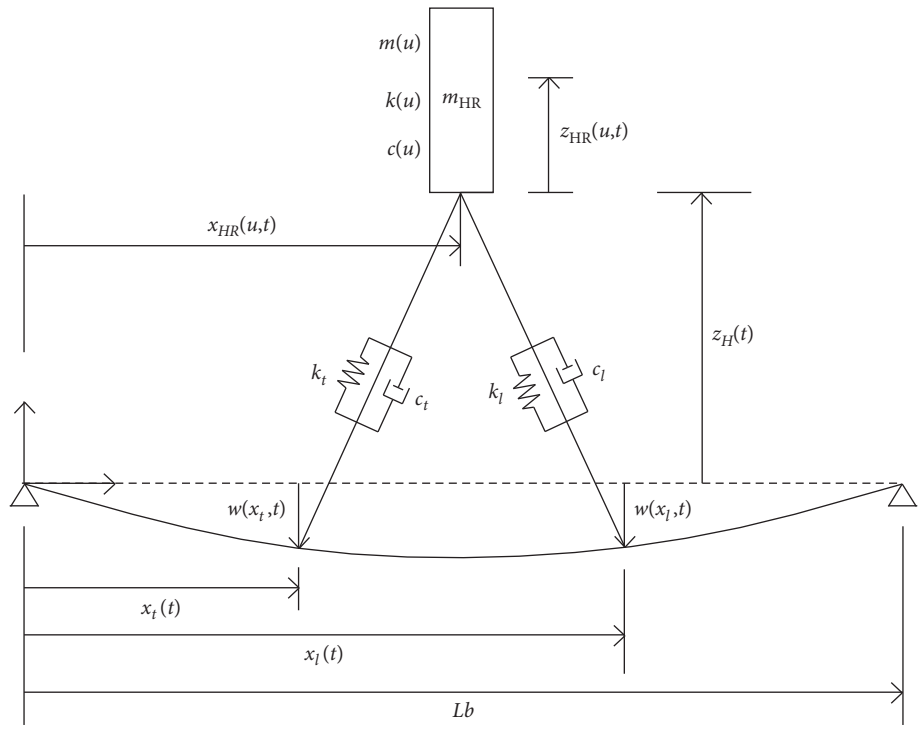

Figure 1: Human-structure interaction bipedal model with the continuum.

The corresponding axial velocity of the two legs can be given as follows:

$$\dot{L}_l(t) = \frac{1}{L_l(t)}\left(\dot{x}_{\mathrm{HR}} L_{lx} + \left(\dot{z}_H - \dot{w}(x_l,t)\right)L_{lz}\right), \tag{5a}$$

$$\dot{L}_t(t) = \frac{1}{L_t(t)}\left(\dot{x}_{\mathrm{HR}} L_{tx} + \left(\dot{z}_H - \dot{w}(x_t,t)\right)L_{tz}\right), \tag{5b}$$

where $L_{lx} = x_{\mathrm{HR}}(t) - x_l$, $L_{tx} = x_{\mathrm{HR}}(t) - x_t$, $L_{lz} = z_H(t) - w(x_l,t)$, and $L_{lz} = z_H(t) - w(x_t,t)$. L_{lx} and L_{tx} denote the horizontal projection of the leading and trailing legs along the x-direction. L_{lz} and L_{tz}denote the vertical projection of the leading and trailing legs along the z-direction. The variations of the leading and trailing legs and the relative vertical displacement of a specific point of the continuum with respect to the base can be denoted as

$$\delta L_l = \frac{\left(\delta z_H - \sum_{j=1}^{n}\phi_j(x_l)\delta Y_j\right)L_{lz}}{L_l} = \frac{\left(\phi_{\mathrm{HR1}}(u)\delta z_{\mathrm{HR1}} + \phi_{\mathrm{HR2}}(u)\delta z_{\mathrm{HR2}} - \sum_{j=1}^{n}\phi_j(x_l)\delta Y_j\right)L_{lz}}{L_l}, \tag{6a}$$

$$\delta L_t = \frac{\left(\delta z_H - \sum_{j=1}^{n}\phi_j(x_l)\delta Y_j\right)L_{tz}}{L_t} = \frac{\left(\phi_{\mathrm{HR1}}(u)\delta z_{\mathrm{HR1}} + \phi_{\mathrm{HR2}}(u)\delta z_{\mathrm{HR2}} - \sum_{j=1}^{n}\phi_j(x_l)\delta Y_j\right)L_{tz}}{L_t}, \tag{6b}$$

$$\delta z_{\mathrm{HR}} = \phi_{\mathrm{HR1}}(u)\delta z_{\mathrm{HR1}} + \phi_{\mathrm{HR2}}(u)\delta z_{\mathrm{HR2}}. \tag{6c}$$

The total virtual work of the pedestrian-structure system results from the damping force of two legs, the continuum, and the beam. Therefore, the variation of virtual work W of the system can be given by

$$\begin{aligned}\delta W &= -\sum_{i=1}^{N} c_l \dot{L}_l(t)\delta L_l(t) - \sum_{i=1}^{N} c_t \dot{L}_t(t)\delta L_t(t) - \int_0^{Lb} c_s \dot{w}'' \delta w'' \mathrm{d}x - \int_0^{H} c_{\mathrm{HR}}(u)\dot{z}_{\mathrm{HR}}(u)\delta z_{\mathrm{HR}}\mathrm{d}u \\ &= \sum_{j=1}^{n} Q_j \delta Y_j + \sum_{i=1}^{N} Q_{z_{\mathrm{HR1}}}\delta z_{\mathrm{HR1}} + \sum_{i=1}^{N} Q_{z_{\mathrm{HR2}}}\delta z_{\mathrm{HR2}} + \sum_{i=1}^{N} Q_z \delta z_H = \sum_{i=1}^{N}\sum_{j=1}^{n}\left(c_l \dot{L}_l(t)\frac{L_{lz}}{L_l}\phi_j(x_l) + c_t \dot{L}_t(t)\frac{L_{tz}}{L_t}\phi_j(x_t)\right)\delta Y_j \\ &\quad - \sum_{j=1}^{n}\left(\int_0^{Lb} c_s\left(\sum_{i=1}^{n}\dot{Y}_i\frac{\mathrm{d}^2\phi_i}{\mathrm{d}x^2}\right)\frac{\mathrm{d}^2\phi_j}{\mathrm{d}x^2}\mathrm{d}x\right)\delta Y_j - \sum_{i=1}^{N}\left(c_l \dot{L}_l(t)\frac{L_{lz}}{L_l} + c_t \dot{L}_t(t)\frac{L_{tz}}{L_t}\right)\delta z_H \\ &\quad - \sum_{i=1}^{N}\int_0^{H} c_{\mathrm{HR}}(u)\left(\phi_{\mathrm{HR1}}(u)\dot{z}_{\mathrm{HR1}} + \phi_{\mathrm{HR2}}(u)\dot{z}_{\mathrm{HR2}}\right)\phi_{\mathrm{HR1}}(u)\mathrm{d}u\delta z_{\mathrm{HR1}} \\ &\quad - \sum_{i=1}^{N}\int_0^{H} c_{\mathrm{HR}}(u)\left(\phi_{\mathrm{HR1}}(u)\dot{z}_{\mathrm{HR1}} + \phi_{\mathrm{HR2}}(u)\dot{z}_{\mathrm{HR2}}\right)\phi_{\mathrm{HR2}}(u)\mathrm{d}u\delta z_{\mathrm{HR2}},\end{aligned} \tag{7}$$

Where c_s represents the damping of the structure, $c_{\mathrm{HR}}(u)$ represents the damping of a certain point of the continuum, and the variables $\{Q_1,\ldots,Q_n,Q^{(1)}_{z_{\mathrm{HR1}}},\ldots,Q_{z_{\mathrm{HR1}}}(N),Q^{(1)}_{z_{\mathrm{HR2}}},\ldots,Q^{(N)}_{z_{\mathrm{HR2}}},Q^{(1)}_z,\ldots,Q^{(N)}_z\}$ represent the generalized forcing functions corresponding to coordinates $\{Y_1,\ldots,Y_n,z^{(1)}_{\mathrm{HR1}},\ldots,z^{(N)}_{\mathrm{HR1}},z^{(1)}_{\mathrm{HR2}},\ldots,z^{(N)}_{\mathrm{HR2}},z^{(1)}_H,\ldots,z^{(N)}_H\}$. The generalized forcing functions can be obtained as follows:

$$Q_j = \sum_{i=1}^{N}\left(c_l \dot{L}_l(t)\frac{L_{lz}}{L_l}\phi_j(x_l) + c_t \dot{L}_t(t)\frac{L_{tz}}{L_t}\phi_j(x_t)\right) - \sum_{j=1}^{n}\left(\int_0^{Lb} c_s\left(\sum_{i=1}^{n}\dot{Y}_i\frac{\mathrm{d}^2\phi_i}{\mathrm{d}x^2}\right)\frac{\mathrm{d}^2\phi_j}{\mathrm{d}x^2}\mathrm{d}x\right), \tag{8a}$$

$$Q_z = -\left(c_l \dot{L}_l(t)\frac{L_{lz}}{L_l} + c_t \dot{L}_t(t)\frac{L_{tz}}{L_t}\right), \tag{8b}$$

$$Q_{z_{\mathrm{HR1}}} = -\sum_{i=1}^{N}\int_0^{H} c_{\mathrm{HR}}(u)\left(\phi_{\mathrm{HR1}}\dot{z}_{\mathrm{HR1}} + \phi_{\mathrm{HR2}}\dot{z}_{\mathrm{HR2}}\right)\phi_{\mathrm{HR1}}(u)\mathrm{d}u, \tag{8c}$$

$$Q_{z_{\mathrm{HR2}}} = -\sum_{i=1}^{N}\int_0^{H}\int c_{\mathrm{HR}}(u)\left(\phi_{\mathrm{HR1}}\dot{z}_{\mathrm{HR1}} + \phi_{\mathrm{HR2}}\dot{z}_{\mathrm{HR2}}\right)\phi_{\mathrm{HR2}}(u)\mathrm{d}u. \tag{8d}$$

The Lagrange equations of the pedestrian-structure system can be given as

$$\begin{cases} \dfrac{\mathrm{d}}{\mathrm{d}t}\left(\dfrac{\partial T}{\partial \dot{Y}_j}\right) + \dfrac{\partial V}{\partial Y_j} = Q_j, \\ \dfrac{\mathrm{d}}{\mathrm{d}t}\left(\dfrac{\partial T}{\partial \dot{z}}\right) + \dfrac{\partial V}{\partial z} = Q_z, \\ \dfrac{\mathrm{d}}{\mathrm{d}t}\left(\dfrac{\partial T}{\partial \dot{z}_{\mathrm{HR1}}}\right) + \dfrac{\partial V}{\partial z_{\mathrm{HR1}}} = Q_{Z_{\mathrm{HR1}}}, \\ \dfrac{\mathrm{d}}{\mathrm{d}t}\left(\dfrac{\partial T}{\partial \dot{z}_{\mathrm{HR2}}}\right) + \dfrac{\partial V}{\partial z_{\mathrm{HR2}}} = Q_{Z_{\mathrm{HR2}}}. \end{cases} \tag{9}$$

Substituting equations (2a)-(2b) and (8a)-(8d) into (9), the equations of motion of pedestrian-structure system can be obtained as follows:

$$M_j\ddot{Y}_j + 2\xi_j\omega_j\dot{Y}_j + M_j\omega_j^2 Y_j + \sum_{i=1}^{N}\sum_{p=1}^{n}\left(C_{ltz}\odot\Phi_{pj}\right)\dot{Y}_p(t) - \sum_{i=1}^{N}\left(C_{ltz}\odot\phi_j\right)\dot{z}_H - \sum_{i=1}^{N}\sum_{p=1}^{n}\left(K_{lt}\odot\Phi_{pj}\right)Y_p(t) + \sum_{i=1}^{N}\left(K_{lt}\odot\phi_j\right)z_H = \sum_{i=1}^{N} C_{lt}\odot L_{xz}\odot\phi_j\dot{x}_{\mathrm{HR}}, \tag{10a}$$

$$m_{\mathrm{HR}}\ddot{z}_H + C_{ltzz}\dot{z}_H - \sum_{i=1}^{N} K_{lltt}z_H + \sum_{j=1}^{n}\left(K_{lt}\odot\phi_j\right)Y_j(t) - \sum_{j=1}^{n}\left(C_{ltzz}\odot\phi_j\right)\dot{Y}_j(t) + m_{\mathrm{HR1}}\ddot{z}_{\mathrm{HR1}} + m_{\mathrm{HR2}}\ddot{z}_{\mathrm{HR2}} = -\left(C_{lt}\odot L_{xz}\right)\dot{x}_{\mathrm{HR}} - m_{\mathrm{HR}}g, \tag{10b}$$

$$m_{\mathrm{HR11}}\ddot{z}_{\mathrm{HR1}} + 2\xi_{\mathrm{HR1}}\omega_{\mathrm{HR1}}m_{\mathrm{HR11}}\dot{z}_{\mathrm{HR1}} + m_{\mathrm{HR1}}\ddot{z}_H + k_{\mathrm{HR1}}z_{\mathrm{HR1}} = -m_{\mathrm{HR1}}g, \tag{10c}$$

$$m_{\mathrm{HR22}}\ddot{z}_{\mathrm{HR2}} + 2\xi_{\mathrm{HR2}}\omega_{\mathrm{HR2}}m_{\mathrm{HR22}}\dot{z}_{\mathrm{HR2}} + m_{\mathrm{HR2}}\ddot{z}_H + k_{\mathrm{HR2}}z_{\mathrm{HR2}} = -m_{\mathrm{HR2}}g, \tag{10d}$$

where ξ_j and ω_j, respectively, denote the damping ratio and circular frequency of the ith vibration mode of the beam in the lateral direction. ω_{HR1}, ω_{HR2}, ξ_{HR1}, and ξ_{HR2} denote the circular frequencies of the first two modes of the continuum and the corresponding damping ratios, respectively. The other variables will be discussed later. The above formula can ultimately be expressed in matrix form:

$$M\ddot{U} + C\dot{U} + KU = P, \tag{11}$$

where M, C, and K are the mass, damping, and stiffness matrices of pedestrian-structure system, respectively. $\ddot{U}$, $\dot{U}$, U, and P are acceleration, velocity, displacement, and forces vector, respectively. If N pedestrians are assumed in the pedestrian-structural model, where the continuum part of each person is considered in its first two modes, then the mass matrix of the kinetic equations can be given as

$$M = \begin{bmatrix} M_1 & \cdots & 0 & & & & & & & \\ \vdots & 0 & \vdots & & & & & & & \\ 0 & \cdots & M_n & & & & & & & \\ & & & m_{\mathrm{HR}}^{(1)} & \cdots & 0 & m_{\mathrm{HR1}}^{(1)} & \cdots & 0 & m_{\mathrm{HR2}}^{(1)} & \cdots & 0 \\ & & & \vdots & 0 & \vdots & \vdots & \ddots & \vdots & \vdots & \ddots & \vdots \\ & & & 0 & \cdots & m_{\mathrm{HR}}^{(N)} & 0 & \cdots & m_{\mathrm{HR1}}^{(N)} & 0 & \cdots & m_{\mathrm{HR2}}^{(N)} \\ & & & m_{\mathrm{HR1}}^{(1)} & \cdots & 0 & m_{\mathrm{HR11}}^{(1)} & \cdots & 0 & & & \\ & & & \vdots & \ddots & \vdots & \vdots & 0 & \vdots & & & \\ & & & 0 & \cdots & m_{\mathrm{HR1}}^{(N)} & 0 & \cdots & m_{\mathrm{HR11}}^{(N)} & & & \\ & & & m_{\mathrm{HR2}}^{(1)} & \cdots & 0 & & & & m_{\mathrm{HR22}}^{(1)} & \cdots & 0 \\ & & & \vdots & \ddots & \vdots & & & & \vdots & 0 & \vdots \\ & & & 0 & \cdots & m_{\mathrm{HR2}}^{(N)} & & & & 0 & \cdots & m_{\mathrm{HR22}}^{(N)} \end{bmatrix}_{(n+3N)\times(n+3N)}. \tag{12}$$

The damping matrix of the kinetic equations of the pedestrian-structure system can be formulated as

$$C = \begin{bmatrix} 2M_1\xi_1\omega_1 + \sum_{i=1}^{N} C_{ltz}\odot\Phi_{11} & \cdots & \sum_{i=1}^{N} C_{ltz}\odot\Phi_{n1} & -C_{ltz}^{(1)}\odot\phi_1 & \cdots & -C_{ltz}^{(1)}\odot\phi_1 & & & & \\ \vdots & \ddots & \vdots & \vdots & \ddots & \vdots & & & & \\ \sum_{i=1}^{N} C_{ltz}\odot\Phi_{1n} & \cdots & 2M_n\xi_n\omega_n + \sum_{i=1}^{N} C_{ltz}\odot\Phi_{nn} & -C_{ltz}^{(N)}\odot\phi_n & \cdots & -C_{ltz}^{(N)}\odot\phi_n & & & & \\ -C_{ltz}^{(1)}\odot\phi_1 & \cdots & -C_{ltz}^{(1)}\odot\phi_n & C_{ltzz} & \cdots & 0 & & & & \\ \vdots & \ddots & \vdots & \vdots & \ddots & \vdots & & & & \\ -C_{ltz}^{(N)}\odot\phi_1 & \cdots & -C_{ltz}^{(N)}\odot\phi_n & 0 & \cdots & C_{ltzz} & & & & \\ & & & & & & C_{\mathrm{HR1}}^{(1)} & & & \\ & & & & & & & \ddots & & \\ & & & & & & & & C_{\mathrm{HR1}}^{(N)} & \\ & & & & & & & & & C_{\mathrm{HR2}}^{(1)} \\ & & & & & & & & & & \ddots \\ & & & & & & & & & & & C_{\mathrm{HR2}}^{(N)} \end{bmatrix}_{(n+3N)\times(n+3N)}. \tag{13}$$

The corresponding stiffness matrix can be expressed as

$$K = \begin{bmatrix} M_1\omega_1^2 - \sum_{i=1}^{N} K_{lt} \odot \Phi_{11} & \cdots & -\sum_{i=1}^{N} K_{lt} \odot \Phi_{n1} & K_{lt}^{(1)} \odot \phi_1 & \cdots & K_{lt}^{(N)} \odot \phi_1 & & & & & & \\ \vdots & \ddots & \vdots & \vdots & \ddots & \vdots & & & & & & \\ -\sum_{i=1}^{N} K_{lt} \odot \Phi_{1n} & \cdots & M_n\omega_n^2 - \sum_{i=1}^{N} K_{lt} \odot \Phi_{nn} & K_{lt}^{(1)} \odot \phi_n & \cdots & K_{lt}^{(N)} \odot \phi_n & & & & & & \\ K_{lt}^{(1)} \odot \phi_1 & \cdots & K_{lt}^{(1)} \odot \phi_n & -K_{lltt}^{(1)} & \cdots & 0 & & & & & & \\ \vdots & \ddots & \vdots & \vdots & \ddots & \vdots & & & & & & \\ K_{lt}^{(N)} \odot \phi_1 & \cdots & K_{lt}^{(N)} \odot \phi_n & 0 & \cdots & -K_{lltt}^{(N)} & & & & & & \\ & & & & & & k_{\mathrm{HR1}}^{(1)} & \cdots & 0 & & & \\ & & & & & & \vdots & \ddots & \vdots & & & \\ & & & & & & 0 & \cdots & k_{\mathrm{HR1}}^{(N)} & & & \\ & & & & & & & & & k_{\mathrm{HR2}}^{(1)} & \cdots & 0 \\ & & & & & & & & & \vdots & \ddots & \vdots \\ & & & & & & & & & 0 & \cdots & k_{\mathrm{HR2}}^{(N)} \end{bmatrix}_{(n+3N)\times(n+3N)}. \tag{14}$$

The displacement vector and the external force vector can be rendered as follows:

$$U = \begin{bmatrix} Y_1 & \cdots & Y_n & Z_H^{(1)} & \cdots & Z_H^{(N)} & Z_{\mathrm{HR1}}^{(1)} & \cdots & Z_{\mathrm{HR1}}^{(N)} & Z_{\mathrm{HR2}}^{(1)} & \cdots & Z_{\mathrm{HR2}}^{(N)} \end{bmatrix}_{1\times(n+3N)}, \tag{15a}$$

$$P = \begin{bmatrix} \sum_{i=1}^{N} C_{lt} \odot L_{xz} \odot \phi_1 \dot{x}_{\mathrm{HR}} \\ \vdots \\ \sum_{i=1}^{N} C_{lt} \odot L_{xz} \odot \phi_n \dot{x}_{\mathrm{HR}} \\ -\left(C_{lt} \odot L_{xz}\right)^{(1)} \dot{x}_{\mathrm{HR}}^{(1)} - m_{\mathrm{HR}}^{(1)} g \\ \vdots \\ -\left(C_{lt} \odot L_{xz}\right)^{(N)} \dot{x}_{\mathrm{HR}}^{(N)} - m_{\mathrm{HR}}^{(N)} g \\ -m_{\mathrm{HR1}}^{(1)} g \\ \vdots \\ -m_{\mathrm{HR1}}^{(N)} g \\ -m_{\mathrm{HR2}}^{(1)} g \\ \vdots \\ -m_{\mathrm{HR2}}^{(N)} g \end{bmatrix}_{(n+3N)\times 1}. \tag{15b}$$

The variables in equations (13) to (15a)-(15b) can be derived as follows:

$$
\begin{aligned}
k_{ll} &= k_l \frac{L_0 - L_l}{L_l},\\
k_{tt} &= k_t \frac{L_0 - L_t}{L_t},\\
C_{lz} &= c_l \left(\frac{L_{lz}}{L_l}\right)^2,\\
C_{tz} &= c_t \left(\frac{L_{tz}}{L_t}\right)^2,\\
C_{lzz} &= c_l \frac{L_{lz}}{L_l},\\
C_{tzz} &= c_t \frac{L_{tz}}{L_t},\\
L_{xzl} &= \frac{L_{lx} L_{lz}}{L_l^2},\\
L_{xzt} &= \frac{L_{tx} L_{tz}}{L_t^2},\\
C_{ltzz} &= \left(c_l \frac{L_{lz}}{L_l} + c_t \frac{L_{tz}}{L_t}\right),\\
C_{lzz} &= c_l \frac{L_{lz}}{L_l},
\end{aligned}
$$

$$
\begin{aligned}
C_{tzz} &= c_t \frac{L_{tz}}{L_t} \phi_j,\\
C_{ltzz} &= C_{lzz} + C_{tzz},\\
K_{lltt} &= k_{ll} + k_{tt},\\
\phi_i(x) &= \sin\left(\frac{i\pi x}{Lb}\right), \quad x\\
\Phi_{pj}(x_l) &= \phi_p(x_l)\phi_j(x_l),\\
\Phi_{pj}(x_t) &= \phi_p(x_t)\phi_j(x_t),\\
C_{ltz} \odot \phi_j &= C_{lz}\phi_j(x_l) + C_{tz}\phi_j(x_t),\\
K_{lt} \odot \phi_j &= k_{ll}\phi_j(x_l) + k_{tt}\phi_j(x_t),\\
K_{lt} \odot \Phi_{pj} &= k_{ll}\Phi_{pj}(x_l) + k_{tt}\Phi_{pj}(x_t),\\
C_{lt} \odot L_{xz} \odot \phi_j &= c_l \frac{L_{lx} L_{lz}}{L_l^2}\phi_j(x_l) + c_t \frac{L_{tx} L_{tz}}{L_t^2}\phi_j(x_t),\\
C_{ltz} \odot \Phi_{pj} &= C_{lz}\Phi_{pj}(x_l) + C_{tz}\Phi_{pj}(x_t),\\
C_{ltz} \odot \phi_j &= C_{lz}\phi_j(x_l) + C_{tz}\phi_j(x_t),\\
K_{lt} \odot \Phi_{pj} &= k_{ll}\Phi_j(x_l) + k_{tt}\Phi_j(x_t),\\
K_{lt} \odot \phi_j &= k_{ll}\phi_j(x_l) + k_{tt}\phi_j(x_t),\\
C_{lt} \odot L_{xz} &= c_l L_{xzl} + c_t L_{xzt},\\
C_{ltzz} \odot \phi_j &= C_{lzz}\phi_j(x_l) + C_{tzz}\phi_j(x_t).
\end{aligned}
\tag{16}
$$

The variables associated with the modes of the system can be expressed as follows:

$$
\begin{aligned}
m_{HR1} &= \int_0^H m(u)\phi_{\mathrm{HR1}}(u)\mathrm{d}u,\\
m_{\mathrm{HR2}} &= \int_0^H m(u)\phi_{\mathrm{HR2}}(u)\mathrm{d}u,\\
m_{\mathrm{HR11}} &= \int_0^H m(u)\phi_{\mathrm{HR1}}^2(u)\mathrm{d}u,\\
m_{\mathrm{HR22}} &= \int_0^H m(u)\phi_{\mathrm{HR2}}^2(u)\mathrm{d}u,\\
m_{\mathrm{HR12}} &= \int_0^H m(u)\phi_{\mathrm{HR1}}(u)\phi_{\mathrm{HR2}}(u)\mathrm{d}u = 0,\\
k_{\mathrm{HR1}} &= \int_0^H k_{\mathrm{HR}}(u)\left(\frac{\mathrm{d}\phi_{\mathrm{HR1}}}{\mathrm{d}u}\right)^2 \mathrm{d}u,\\
k_{\mathrm{HR2}} &= \int_0^H k_{\mathrm{HR}}(u)\left(\frac{\mathrm{d}\phi_{\mathrm{HR2}}}{\mathrm{d}u}\right)^2 \mathrm{d}u,\\
k_{\mathrm{HR12}} &= \int_0^H k_{\mathrm{HR}}(u)\frac{\mathrm{d}\phi_{\mathrm{HR2}}}{\mathrm{d}u}\frac{\mathrm{d}\phi_{\mathrm{HR1}}}{\mathrm{d}u}\mathrm{d}u = 0,\\
C_{\mathrm{HR1}} &= 2m_{\mathrm{HR11}}\omega_{\mathrm{HR1}}\xi_{\mathrm{HR1}} = \int_0^H c_{\mathrm{HR}}(u)\phi_{\mathrm{HR1}}^2(u)\mathrm{d}u,\\
C_{\mathrm{HR2}} &= 2m_{\mathrm{HR22}}\omega_{\mathrm{HR2}}\xi_{\mathrm{HR2}} = \int_0^H c_{\mathrm{HR}}(u)\phi_{\mathrm{HR2}}^2(u)\mathrm{d}u,\\
C_{\mathrm{HR12}} &= \int_0^H c_{\mathrm{HR}}(u)\phi_{\mathrm{HR1}}\phi_{\mathrm{HR2}}(u)\mathrm{d}u = 0.
\end{aligned}
\tag{17}
$$

From the above derivation, it can be noted that the mass coupling of the continuum is included in the M matrix, so that the mass matrix tends to show diagonal trends and partial intercoupling. It is noteworthy that, in the damping matrix C, the damping of the legs is coupled to the damping of the structure, with the feature that the damping element of the legs is spread over the whole matrix. It suggests that the damping of the legs exerts an impact on the damping of the system. The continuum is not coupled to other damping terms in the damping matrix due to the relative coordinates adopted. After performing an absolute coordinate transformation, however, the damping of the continuum is also coupled to other damping terms in the damping matrix C. Because the transformations are not the focus of the study, relevant details are not discussed here. As similar to the damping matrix, the distribution of the stiffness elements in the stiffness matrix K is characterized by the fact that the structural, bipedal, and continuum stiffness are coupled to each other, which demonstrates the contribution of the three components to the stiffness of the entire system. It should be noted that although the overall matrix bears a resemblance to Gao's [30] and Qin's [27, 28] models, their models treat the human body as a concentrated mass and ignore the influence of mass, stiffness, and damping distribution of other body parts. Therefore, their models fail to measure the effects of the bipedal models, as well as the continuum, on

the entire pedestrian-structural system, which makes a clear distinction between the new model proposed and theirs. It is manifested in the mass matrix M by the addition of $m_{\mathrm{HR11}}^{(p)}$, $m_{\mathrm{HR22}}^{(p)}$, $m_{\mathrm{HR1}}^{(p)}$, and $m_{\mathrm{HR2}}^{(p)}$ in the damping matrix C by the addition of $C_{\mathrm{HR1}}^{(p)}$ and $C_{\mathrm{HR2}}^{(p)}$ and in the stiffness matrix K by the addition of $k_{\mathrm{HR1}}^{(p)}$ and $k_{\mathrm{HR2}}^{(p)}$ compared to the model proposed by Gao and Yang [30]. The new model can obtain vibration response along the standing human body by taking appropriate parameters and allows for the possibility to perform correlated gait adjustments through the perceived acceleration of the human body, which reveals the limitation of classic models with a focus on the concentrated mass.

2.3. Damping and Stiffness Definition of Legs during a Gait Cycle. The derivation of the formula discussed in Part 2.2 is assumed on the case where a pedestrian's two legs are in contact with the ground. In the process of pedestrian gait, the switch between the leading and trailing legs is the primary cause of GRF. In the process of gait transition, there exist cases where one leg is not in touch with the structure. To assume the single-leg contact as a special case of double-leg contact, we set the parameter of stiffness of the corresponding leg to zero. This approach enables the matrix dimension of the dynamic equations to be kept constant across different gait phases, which reduces the types of variables and decreases the complexity of the calculations. k_{leg} denotes the total stiffness of one leg, which is assumed to maintain a constant state for the duration of a gait cycle in this study.

The paper argues that once the leading foot touches the ground, the leg stiffness that corresponds to the model should be minimal due to the bending motion of the ankles. In a similar manner, the stiffness of the trailing leg can be assumed minimal when the trailing foot is off the ground. To explore the impact of variable stiffness on the relevant dynamics results, two different approaches are employed to define stiffness as equations (18a) and (18b). Equation (18a) ignores the variations of stiffness, which shows that the stiffness of the legs remains invariable throughout the gait cycle. Equation (18b), however, defines the base stiffness k_{leg1}, in which the remaining stiffness k_{leg2} is distributed according to the relative compression of the two legs. The effect of $\eta = (k_{\mathrm{leg2}}/k_{\mathrm{leg1}})$ (the relative ratio of k_{leg2} and k_{leg1}) on the structural response can be explored through the application of variable stiffness strategies. The stiffness strategies are taken as follows:

$$\begin{cases} k_l = k_{\mathrm{leg}}, k_t = k_{\mathrm{leg}}, & L_l < L_0, L_t < L_0, \\ k_l = k_{\mathrm{leg}}, k_t = 0, & L_l < L_0, L_t \geq L_0, \\ k_l = 0, k_t = k_{\mathrm{leg}}, & L_l \geq L_0, L_t < L_0, \end{cases} \tag{18a}$$

$$\begin{cases} k_l = k_{\mathrm{leg1}} + \dfrac{L_0 - L_l}{2L_0 - L_l - L_t} k_{\mathrm{leg2}}, & \\ & L_l < L_0, L_t < L_0, \\ k_t = k_{\mathrm{leg1}} + \dfrac{L_0 - L_t}{2L_0 - L_l - L_t} k_{\mathrm{leg2}}, & \\ k_l = k_{\mathrm{leg1}} + k_{\mathrm{leg2}}, k_t = 0, & L_l < L_0, L_t \geq L_0, \\ k_l = 0, k_t = k_{\mathrm{leg1}} + k_{\mathrm{leg2}}, & L_l \geq L_0, L_t < L_0. \end{cases} \tag{18b}$$

Meanwhile, to guarantee that the total damping of the human leg remains invariable during the gait cycle, the damping is distributed based on the proportion of compression of the two legs. c_{leg} denotes the total damping of the legs, which is assumed to be a fixed constant in the gait cycle in this paper. The damping distribution strategies are obtained as

$$\begin{cases} c_l = \dfrac{L_0 - L_l}{2L_0 - L_l - L_t} c_{\mathrm{leg}}, & \\ & L_l < L_0, L_t < L_0, \\ c_t = \dfrac{L_0 - L_t}{2L_0 - L_l - L_t} c_{\mathrm{leg}}, & \\ c_l = c_{\mathrm{leg}}, c_t = 0, & L_l < L_0, L_t \geq L_0, \\ c_l = 0, c_t = c_{\mathrm{leg}}, & L_l > L_0, L_t \leq L_0. \end{cases} \tag{19}$$

2.4. GRF during a Gait Cycle. The interaction force between the leg and the structure consists of two parts: the elastic force generated by the spring and the damping force generated by the damping. F_l indicates the interaction force between the leading leg and the structure, and F_t indicates the interaction force between the trailing leg and the structure. F_{lx} and F_{tx} denote the horizontal projection values of the interaction forces of the leading and trailing legs with the structure, respectively. F_{lz} and F_{tz} denote the vertical projection values of the interaction forces of the

leading and trailing legs with the structure, respectively. The components of GRF in both directions and the associated variables can be expressed as follows:

$$
\begin{aligned}
&F_l = K_l\left(L_0 - L_l\right) + c_l\dot{L}_l,\\
&F_t = K_t\left(L_0 - L_t\right) + c_t\dot{L}_t,\\
&F_{lx} = F_l\cos\theta = F_l\frac{L_{lx}}{L_l} = \left[K_l\left(L_0 - L_l\right) + c_l\frac{1}{L_l}\left(\dot{x}_{\mathrm{HR}}L_{lx} + \left(\dot{z}_H - \dot{w}\left(x_l,t\right)\right)L_{lz}\right)\right]\\
&\frac{L_{lx}}{L_l} = K_{ll}L_{lx} + C_{lx}\dot{x}_{\mathrm{HR}} + c_lL_{xzl}\left(\dot{z}_H - \dot{w}\left(x_l,t\right)\right), F_{tx} = K_{tt}L_{tx} + C_{tx}\dot{x}_{\mathrm{HR}} + c_tL_{xzt}\left(\dot{z}_H - \dot{w}\left(x_t,t\right)\right),\\
&F_{lz} = F_l\frac{L_{lz}}{L_l} = \left[K_l\left(L_0 - L_l\right) + c_l\frac{1}{L_l}\left(\dot{x}_{\mathrm{HR}}L_{lx} + \left(\dot{z}_H - \dot{w}\left(x_l,t\right)\right)L_{lz}\right)\right]\\
&\frac{L_{lz}}{L_l} = K_{ll}L_{lz} + c_lL_{xzl}\dot{x}_{\mathrm{HR}} + C_{lz}\left(\dot{z}_H - \dot{w}\left(x_l,t\right)\right),\\
&F_{tz} = K_{tt}L_{tz} + c_tL_{xzt}\dot{x}_{\mathrm{HR}} + C_{tz}\left(\dot{z}_H - \dot{w}\left(x_t,t\right)\right),\\
&C_{lx} = c_l\left(\frac{L_{lx}}{L_l}\right)^2,\\
&C_{tx} = c_t\left(\frac{L_{tx}}{L_t}\right)^2.
\end{aligned}
\tag{20}
$$

3. Dynamic Analysis of Structure

The dynamics properties of the coupled pedestrian-structure system shift over time in pedestrians' walking process. The dominant modes of this pedestrian-structure interaction system are closely related to the modes of the uncoupled structure and the human body at any instant of time. Therefore, a modal analysis is essential to track the dynamics of the coupled system. The instantaneous frequencies and damping ratios of the system will vary with the fluent interaction between pedestrians and structure. The instantaneous modal properties of the system are determined by means of the state-space method [33] as

$$
\begin{aligned}
&\dot{\Psi} = A\Psi + B,\\
&\Psi = \begin{pmatrix} U \\ \dot{U} \end{pmatrix},\\
&A = \begin{bmatrix} 0 & I \\ -M^{-1}K & -M^{-1}C \end{bmatrix},\\
&B = \begin{pmatrix} 0 \\ M^{-1}P \end{pmatrix},
\end{aligned}
\tag{21}
$$

where I denotes the identity matrix with the same dimension as the stiffness, mass, and damping matrix of the HSI system.

Then the dynamics of the coupled system can be obtained by solving the eigenvalue problem:

$$
A\varphi = \lambda\varphi, \tag{22}
$$

where λ and φ denote the complex eigenvalue and the corresponding eigenvector of matrix A, respectively. Given that A is a time-variant matrix, the corresponding eigenvalues and eigenvectors are time-variant as well. For multi-degree-of-freedom (multi-DOF) damping systems, the ith frequency f_i and the corresponding damping ratio ξ_i can be derived as follows:

$$
\begin{aligned}
f_i &= \frac{1}{2\pi}\left|\lambda_i\right|,\\
\xi_i &= \frac{\mathrm{Re}\left(\lambda_i\right)}{\left|\lambda_i\right|}.
\end{aligned}
\tag{23}
$$

4. Computation Procedure

As the modes of the structure and the corresponding damping ratio can be obtained from modal analysis or experimental testing before the computation, we can set the parameters as mass M_i, frequency f_i, shape function φ_i, and damping ratio ξ_i. The initial kinetic parameters of the bipedal model consist of the modal mass (m_{HR1}, m_{HR2}, m_{HR11}, and m_{HR22}), frequencies (ω_{HR1} and ω_{HR2}), corresponding

damping ratios (ξ_{HR1} and ξ_{HR2}) of the continuum, stiffness of the legs k_{leg}, and damping ratio of the legs c_{leg}. The initial gait parameters of the bipedal model include walking velocity $\dot{x}_{HR}$, stride length L_s, leg length L_0, and the position of the initial leading and trailing legs (L_{l0}, L_{t0}) on the structure. Based on the bipedal model proposed in the paper, the calculations can be performed according to the flowchart in Figure 2.

5. Numerical Validation

A simply supported beam with a span of 11.0 m is intended for the simulation [34]. The simple beam has a width of 1.25 m, a thickness of 0.35 m, a section flexural stiffness of $EI = 1.64 \times 10^8\ N \cdot m^2$, and mass per unit length of $\overline{m} = 1.364 \times 10^3$ kg/m and damping ratio $\xi = 0.003$. The fundamental frequency of the beam is 4.51 Hz and the corresponding modal mass is 7040 kg. During the simulation, a pedestrian is assumed to move at a constant velocity from the left end to the right end of the beam, and the bridge is permitted to vibrate freely. The premise of the assumption is that the pedestrian's trailing leg is located at the origin of coordinates and the leading leg is one stride ahead of the trailing leg. Two different stiffness strategies are adopted in this paper, and the parameters of the bipedal walking model are shown in Table 1.

As the response of the simply supported beam at the mid-span under external load is larger as compared to other positions of the beam, the dynamic responses at the mid-span of the beam can be utilized to evaluate the effect of this bipedal model on the structure. To examine the impact of the new model that introduces the concept of continuum on the structural response, a comparison between the new model and Gao's [29] is necessary. From Part 4, it is noted that the appropriate variables U_0 should be determined before calculation. Since this differential equation is time-varying and nonlinear, the initial vector U_0 is crucial to achieve a stable gait in the shortest time possible. To compare Gao's model and the model proposed in the paper in terms of their efficiency to achieve a stable gait, we set the initial acceleration vector to $U_0 = [0\ 1\ 0\ 0]$ (Gao's model) and $U_0 = [0\ 1\ 0\ 0\ 0\ 0]$ (new model), respectively. From Figures 3 and 4, it can be concluded that, under the identical initial conditions, the new model is more efficient in obtaining a stable gait than Gao's, which indicates that an improvement of the stabilization of the bipedal walking model is possible to make if the degrees of freedom of the continuum are taken into account. It is noteworthy that the difference between the two models is very slight in terms of the response of the beam at mid-span after the gait reaches its stability, which is further illustrated in Figures 5 and 6. The phenomenon proves that the model with a continuum does not thoroughly change the dynamics of the bipedal model, which validates the proposed model results.

Therefore, in order to compare the impact of the two models on the dynamic properties of the structure, the acceleration vector is adopted as the initial vector for calculation only after the gait obtains its stabilization. The acceleration and displacements of the beam at mid-span are shown in Figures 7 and 8, respectively, under the condition that the initial vector is optimized. As can be seen from Figure 7, the response of the structure under human-induced loads decreases when the dynamic properties of the continuum are considered, which is evident from the sharp decline in the peak frequencies in Figure 9 as well. The existence of the pedestrian has a reduced effect on the vertical frequency of the structure, and the impact is more prominent when the pedestrian reaches the middle of the structure (Figure 10). In contrast, Figure 11 illustrates that, as a consequence of the coupling between the leg's damping and the structure's damping, the damping ratio of the structure increases. There are minor distinctions between the vertical and longitudinal GRFs of the two models, as illustrated in Figures 12 and 13. The spectrum of mid-span acceleration in Figure 12 suggests that the multiples of the step frequency require special attention, corresponding to the highest spectral peak at $3f_S$, which is close to the fundamental frequency of the structure.

6. Model Parametric Analysis

As noted above, we take two approaches to define leg stiffness, corresponding to equations (18a) and (18b). In Section 5, with the aim at comparing the impact of the two bipedal models on the dynamic properties of the structure, the stiffness definition corresponding to (18a) is adopted; that is, the stiffness of the leg is a constant value throughout the process when the leg is in contact with the structure. In the analysis of the model parameters in the following sections, the definition of stiffness corresponding to equation (18b) is adopted; that is, the stiffness varies with the gait. To facilitate the assessment of the two definitions of stiffness, the sum of k_{leg1} and k_{leg2} is defined as k_{leg} and the ratio of k_{leg1} to k_{leg2} is taken as η (i.e., $\eta = (k_{leg1}/k_{leg2})$). The change in spring stiffness and leg damping in a full gait cycle is shown in Figure 14. In the single-support phase, the stiffness and damping of the hinge leg are kept constant, whereas in the double-support phase, the stiffness and damping of the hinge and swing leg are distributed based on the compression ratio of the two legs. It is notable that, in the single-support phase, both the stiffness and damping of the swing leg have no contribution to the system.

The stiffness, leg damping, and body mass in bipedal walking models are proved to have a significant effect on the dynamic response of the structure [27]. Previous studies [31] have shown that both the dynamics and gait parameters of the bipedal model influence the dynamic response and characteristics of the structure, and the relationship between the two has also been explored. However, these studies have ignored the impact of the dynamics of other parts of the human body (corresponding to the continuum of this model) on the structural response and properties. This paper defines variable stiffness to allow the model to be more compatible with the gait process. The research in [37] has shown that the parameters of the human model are discrete, so the numerical analysis will be conducted in this section to explore the influence of the parameters of each part of the human body on the HSI system. With the control variate

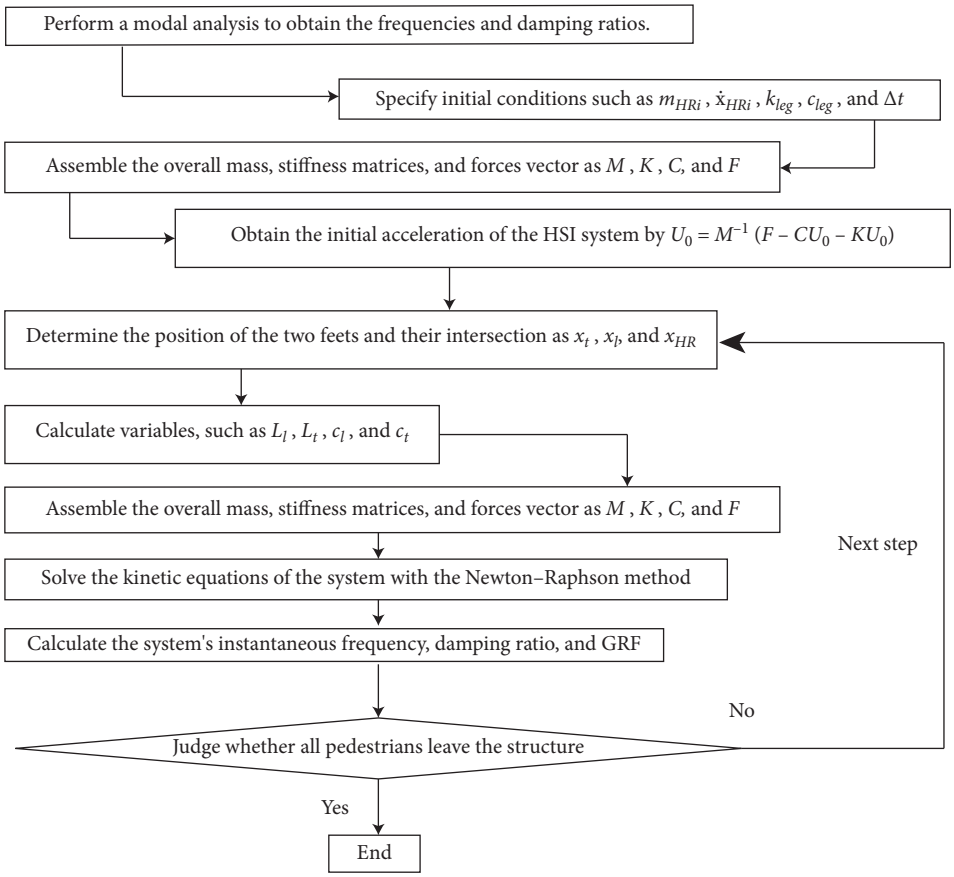

Figure 2: Flowchart of calculation.

Table 1: Parameters of the bipedal walking model.

Model parameters	Value	Unit	References
m_{HR}	74.9	kg	[35]
m_{HR1}	39.9	kg	
m_{HR2}	22.2	kg	
m_{HR11}	29.3	kg	
m_{HR22}	36.5	kg	
k_{HR1}	39844	N/m	[36]
k_{HR2}	320064	N/m	
ω_{HR1}	36.93	rad/s	[35]
ω_{HR2}	93.57	rad/s	
L_0	1.00	m	
k_{leg}	$13.69\dot{x}_{\mathrm{HR}} + 1.587$	kN/m	[37]
ξ_{leg}	$0.045\dot{x}_{\mathrm{HR}} - 0.019$	1	
ξ_{HR1}	0.3	1	
ξ_{HR2}	0.5	1	
L_s	$0.105\dot{x}_{\mathrm{HR}} + 0.513$	m	
$\dot{x}_{\mathrm{HR}}$	1.05	m/s	

method, the parameters of the system are selected based on Table 1, except for some parameters that are required to be studied within a certain range. During the study of the effect of body mass on the results of correlation analysis, the modal masses corresponding to the continuum are all linearly related to the total mass to simplify the calculations; that is, $m_{\mathrm{HR}i}/m_{\mathrm{HR}} = C_{1i}$, $m_{\mathrm{HR}ii}/m_{\mathrm{HR}} = C_{2i}$ $(i = 1, 2)$, with constants C_{1i} and C_{2i}. The ranges of the critical parameters and variables that need to be examined are shown in Table 2.

6.1. The Effects of Continuum Damping and Leg Damping. The additional damping of the pedestrian-structure interaction system is derived from the damping of the legs and

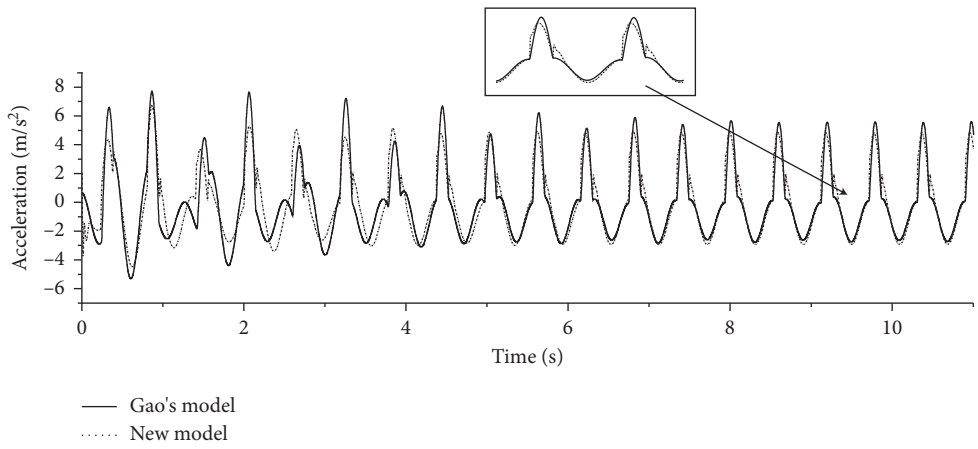

Figure 3: Acceleration of the COM in walking (initial vector not optimized).

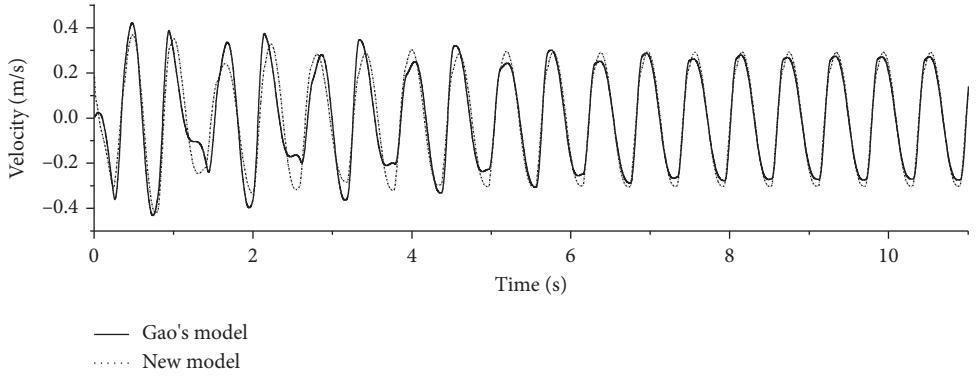

Figure 4: Velocity of the COM in walking (initial vector not optimized).

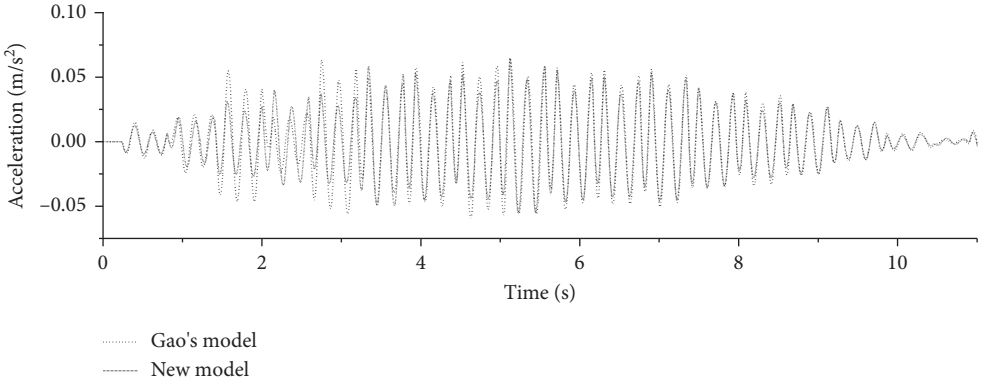

Figure 5: Acceleration of the beam at mid-span (initial vector not optimized).

the continuum. As can be seen from Figure 15, the damping of the continuum affects the damping of the structure with different leg damping ratio ranges. When $\xi_{leg} < 0.07$ and $\xi_{leg} > 0.0283$, the acceleration response of the structure presents a decline tendency at first and then rises with the continuum damping ratio increasing incrementally. When $\xi_{leg} \geq 0.07$, with the increase of continuum damping, the acceleration response correspondingly shows a climbing trend. Figure 16 evidently informs that there are positive correlations between the leg damping and structural acceleration. However, leg damping has an influential effect on the structural damping ratio relative to continuum damping. Only when the leg damping is substantial does the continuum damping have a discernible effect on the structural damping ratio. Contrary to the case where leg damping can noticeably increase the damping ratio of the structure, an increase in leg damping will lead to the reduction of the frequency of the beam, as illustrated in Figure 17. Meanwhile, the damping of the continuum shows a negative correlation with the frequency of the structure,

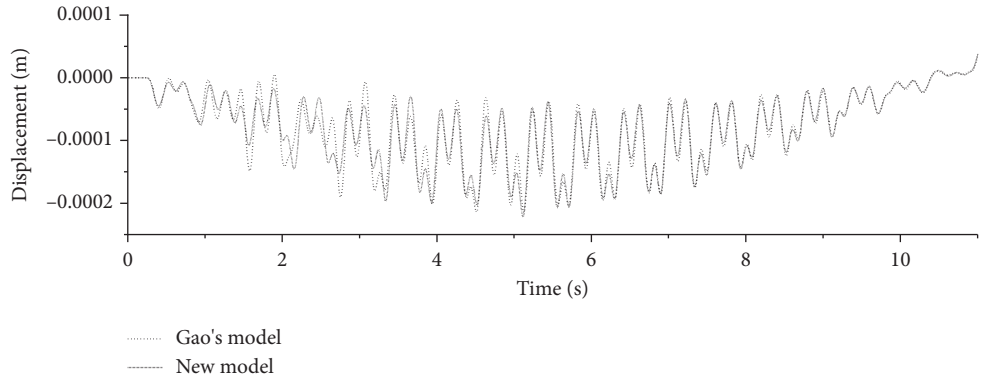

Figure 6: Displacement of the beam at mid-span (initial vector not optimized).

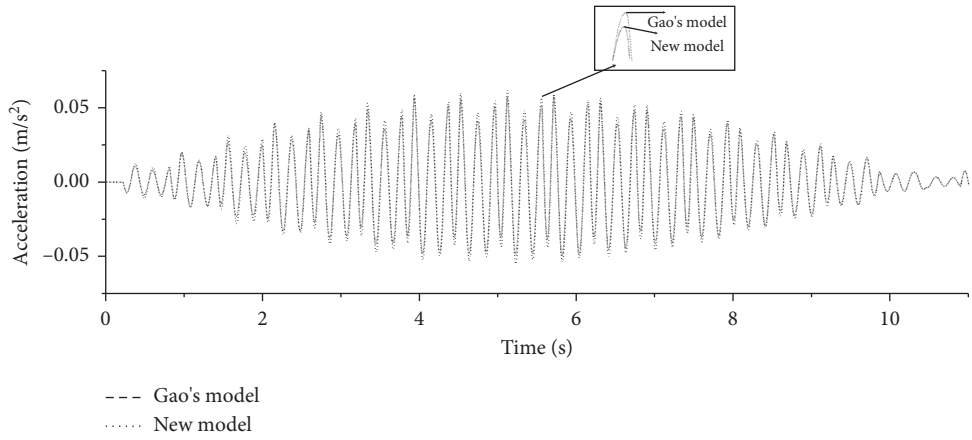

Figure 7: Acceleration at beam mid-span (initial vector optimized).

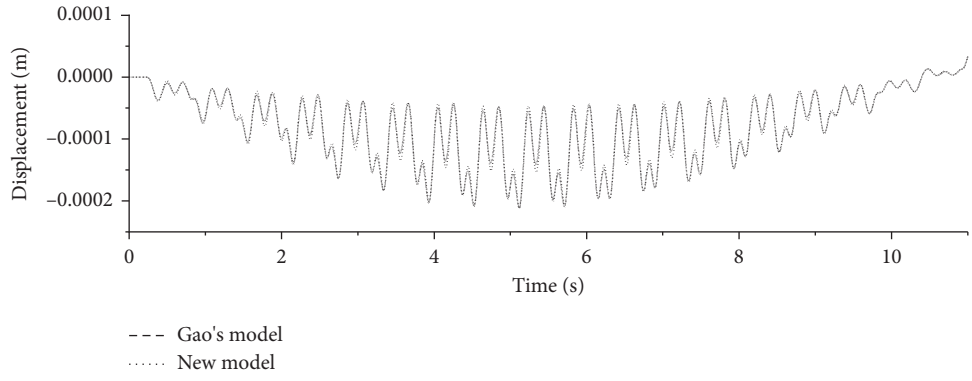

Figure 8: Displacement at beam mid-span (initial vector optimized).

which is more obvious if the damping ratio of the legs is higher (Figure 17).

To examine the effect of different model parameters on GRF, we normalize GRF as GRF/G (normalized GRF), where G refers to the weight of the human body. The damping ratio of the continuum in Figure 18 has a negligible effect on the normalized GRF with fixed leg stiffness $k_{\text{leg}} = 18\,\text{kN/m}$, continuum damping ratio $\xi_{\text{HR}} = 0.5$, stiffness ratio $\eta = 0.3$, and human mass $m_{\text{HR}} = 75\,\text{kg}$. With the increasing leg damping, the first peak of GRF presents a tendency to go down gradually, and there is an obvious slight downward trend in its second peak, which is depicted by Figure 19.

Numerical investigations on the effects of leg and continuum damping on structural properties, response, and GRF show that both leg and continuum damping are effective in increasing the damping and decreasing the frequency of the structure, but leg damping has a stronger impact on GRF than continuum damping does.

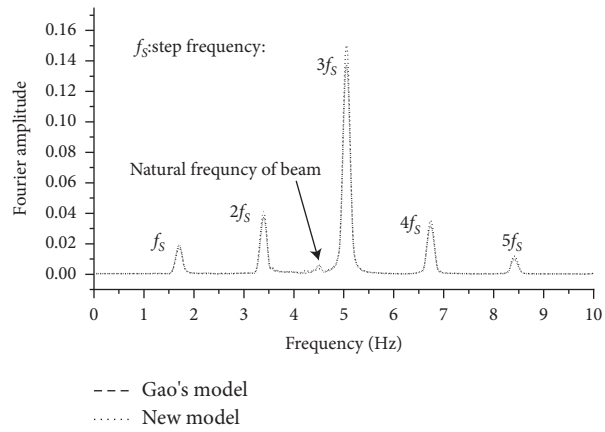

Figure 9: Spectrum of mid-span acceleration.

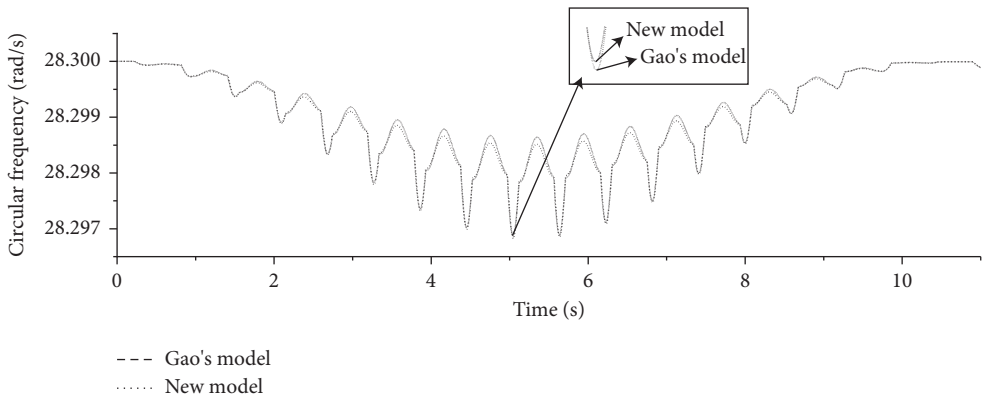

Figure 10: Frequency of the system (initial vector optimized).

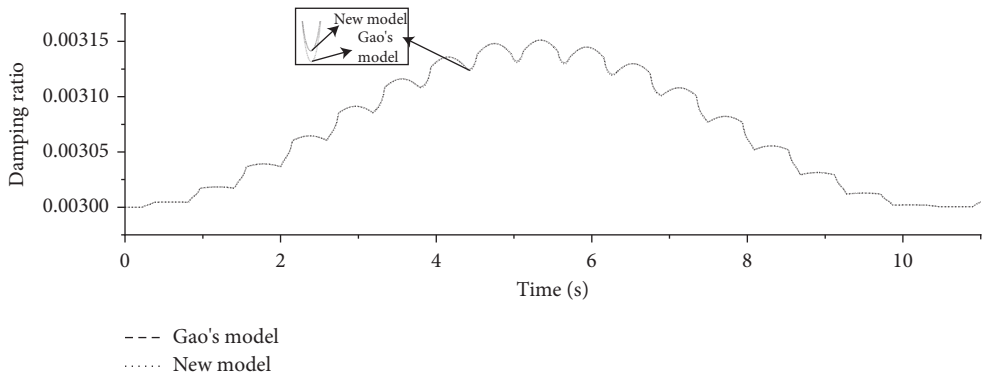

Figure 11: Damping ratio of the system (initial vector optimized).

6.2. The Effects of Human Mass, Leg Damping, and Continuum Damping. Relative to the damping of the legs and continuum, the mass of the body has a much more prominent effect on the response of the structure and its dynamic properties. Figure 20 shows that a larger continuum damping results in a more obvious acceleration response, and the mass of the human body has a larger effect than other parameters and is positively correlated with structural acceleration. Unlike the case shown in Figure 20, where continuum damping is always positively correlated with the structural acceleration response, the model in Figure 21 demonstrates that when the body mass is relatively small (e.g., $50 \le m_{\mathrm{HR}} \le 65$), there is a positive interrelation between the leg damping and structural acceleration, whereas when the body mass is larger (e.g., $85 \le m_{\mathrm{HR}} \le 100$), the acceleration of the structure instead reduces as the leg damping increases. When $70 \le m_{\mathrm{HR}} \le 80$, the leg damping has little effect on the response of the structure. Figure 20 is consistent

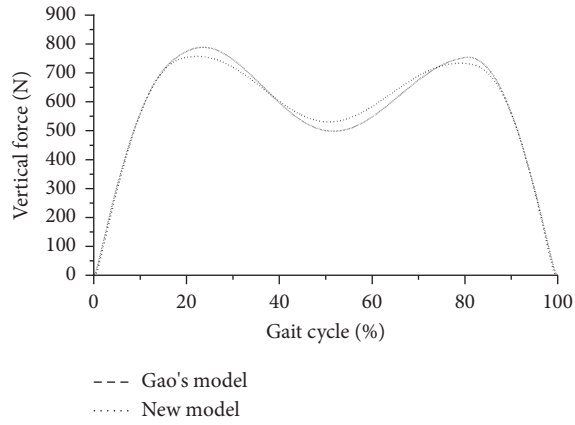

Figure 12: Vertical GRF.

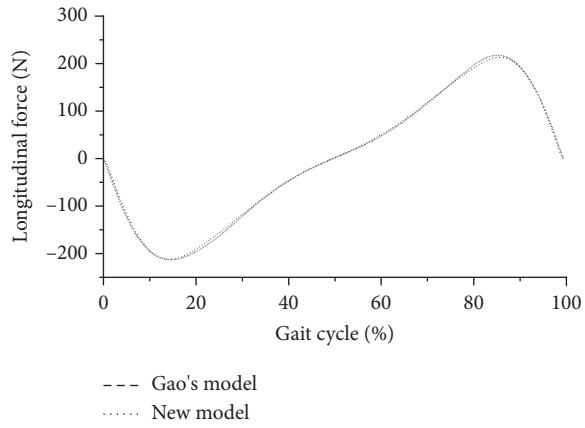

Figure 13: Longitudinal GRF.

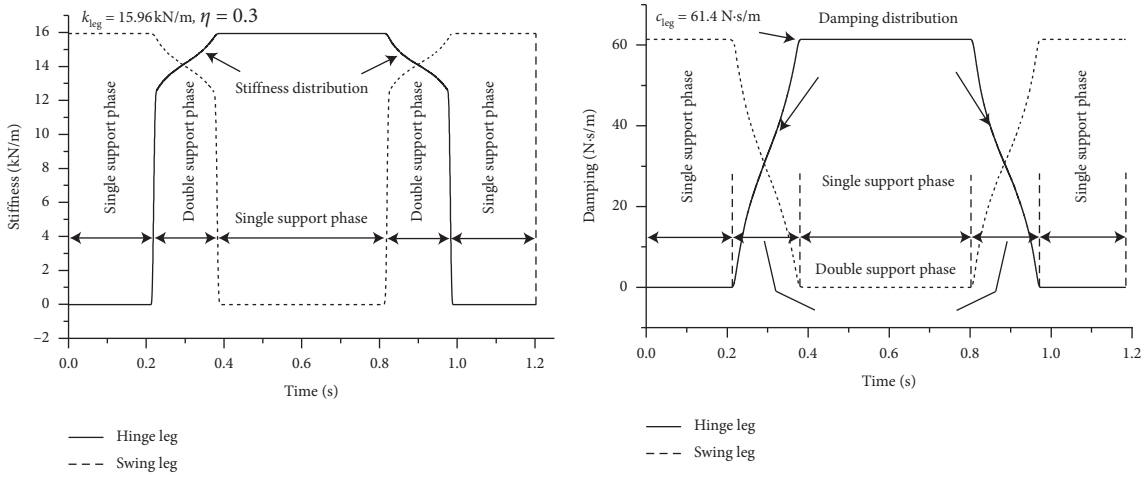

Figure 14: (a) Leg stiffness coefficients. (b) Leg damping coefficients.

with the results shown in Figure 21 in that the mass of the human body has a remarkable effect on the acceleration response of the structure.

The frequency of the structure is negatively correlated with the body mass (Figures 22 and 23), which is consistent with the empirical formula $\omega_s = \sqrt{(k_s/m_s)}$. The damping of

Table 2: Parameters and variable ranges of the bipedal walking model.

Model parameters	Value/value range	Interval	Unit
m_{HR}	50–100	5	kg
m_{HR1}	26.3–53.3	2.66	kg
m_{HR2}	11.8–29.6	1.48	kg
m_{HR11}	19.6–39.1	1.96	kg
m_{HR22}	24.4–48.7	2.44	kg
k_{HR1}	39844	—	N/m
k_{HR2}	320064	—	N/m
ω_{HR1}	36.93	—	rad/s
ω_{HR2}	93.57	—	rad/s
L_0	1.00	—	m
k_{leg}	$13.69\dot{x}_{HR} + 1.587$	2	kN/m
ξ_{leg}	$0.045\dot{x}_{HR} - 0.019$	0.05	1
ξ_{HR1}	0.1–0.5	0.1	1
ξ_{HR2}	0.1–0.5	0.1	1
L_s	$0.105\dot{x}_{HR} + 0.513$	—	m
$\dot{x}_{HR}$	1.05	—	m/s

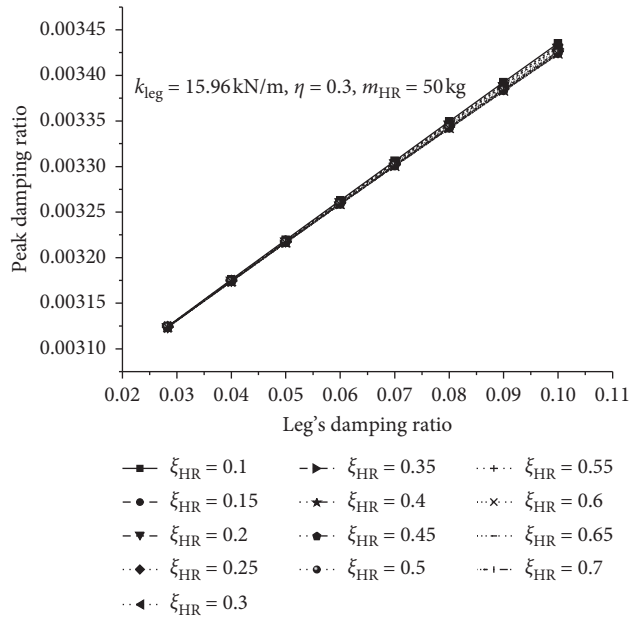

Figure 15: Peak damping ratio of structure under leg stiffness 15.96 kN/m, $\eta = 0.3$, $m_{HR} = 50$ kg, and $\xi_{leg} = 0.05$.

the continuum has a negligible effect on the frequency of the structure (Figure 22), and as the damping of the legs increases, the frequency of the structure decreases correspondingly (Figure 23). Although Figures 24 and 25 affirm the body mass's impact on the structural damping ratio, the effect of continuum damping in fact is negligible. Meanwhile, the more damping in the legs is produced, the more significant effect of body mass is caused on the structure. Therefore, the body mass shows a positive correlation with the structural damping.

From Figure 26, the influence of human mass on GRF can be concluded as follows:

(1) The greater the mass is, the shorter the duration of the impact on the structure at each step is, namely, the shorter GRF period

(2) The greater the mass is, the larger the two peak values are, the more gaps between the crest and the trough are, and the more distinct the M-shaped feature of the GRF shape is

(3) The greater the mass is, the further forward the position of the trough in the graph is

6.3. The Effects of Human Mass, Leg Stiffness, and Damping. The study confirms that the mutual coupling between the human mass, leg stiffness, and damping is not negligible to examine the effect of the bipedal model on structural response and dynamic performance. Figure 27 informs that the effect of leg stiffness on the acceleration response of a structure can be divided into two cases. The first case

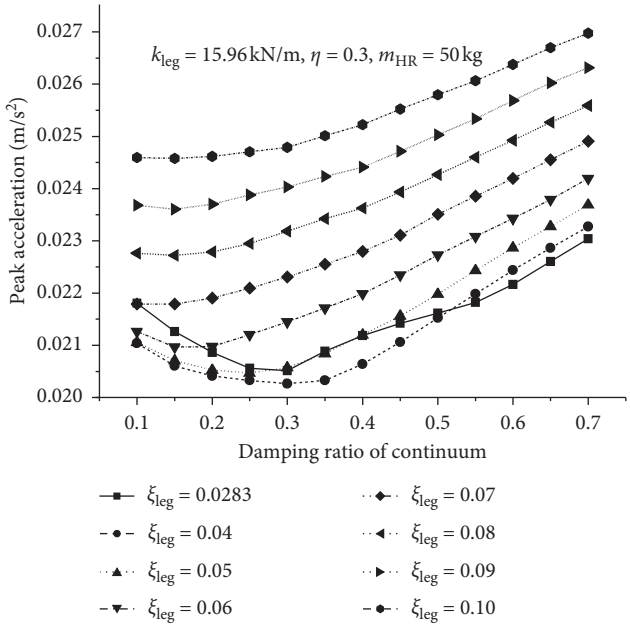

Figure 16: Peak acceleration under leg stiffness 15.96 kN/m, η = 0.3, m_{HR} = 50 kg, and ξ_{HR} = 0.5.

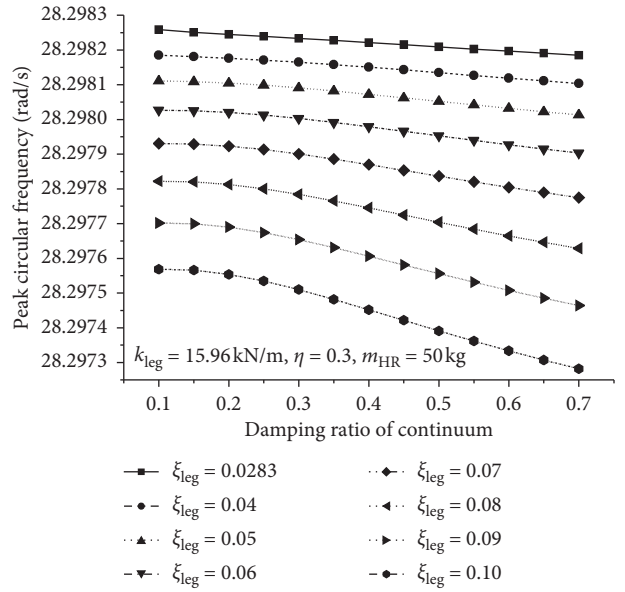

Figure 17: Peak frequency of structure under leg stiffness 15.96 kN/m, η = 0.3, and m_{HR} = 50 kg.

corresponds to the condition when $50 \le m_{HR} < 70$ and $95 \le m_{HR}$, and the higher the leg stiffness is, the smaller the response of the structure is induced. The second case corresponds to the condition when $70 < m_{HR} < 90$, and the stiffness of the leg is positively interrelated with the response of the structure. It is noticeable that the structural response induced by different stiffnesses of the human leg displays a U-shaped trend as the body mass increases. When k_{leg} = 15.96 kN/m, it follows an inverted U shape. The other higher stiffnesses depict a pattern of a "positive U″ shape, and the corresponding troughs offset in the direction of the growing mass with the increased stiffness.

As can be seen in Figure 28, the effect of human leg stiffness on structural frequency can also be divided into two phases. When $50 \le m_{HR} < 60$, leg stiffness is negatively correlated with the frequency of the structure, but when $m_{HR} > 60$, leg stiffness is positively correlated with the frequency of the structure. The correlation between human leg stiffness and structural damping is not as complex as that between human leg stiffness and structural response. As is evident from Figure 29, the damping of the structure has consistently been positively correlated with the damping of the legs. The analysis results presented in Figures 27–29 are all conducted under the following parameters:

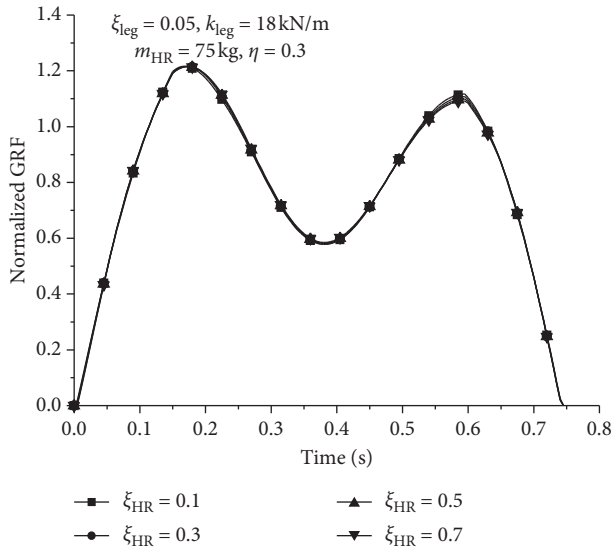

Figure 18: Normalized GRF under different continuum damping ratio.

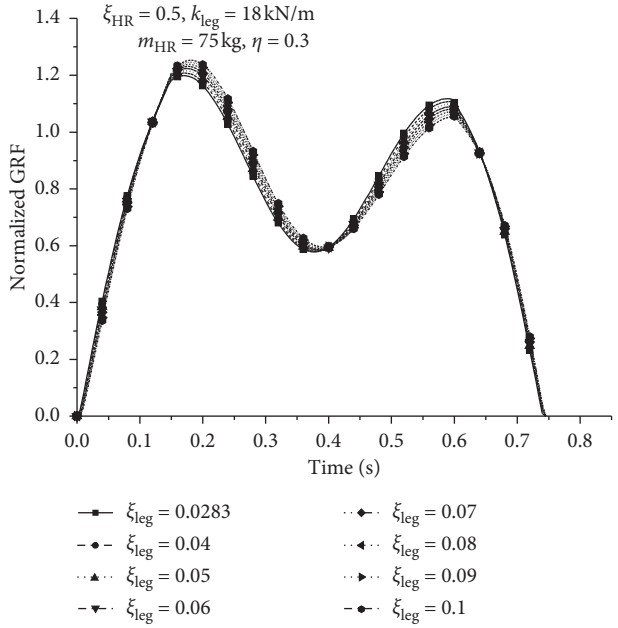

Figure 19: Normalized GRF under different leg damping ratio.

$k_{leg} = 15.96$ kN/m, $\eta = 0.3$, $\xi_{HR} = 0.5$, and $\xi_{leg} = 0.05$. Figure 30 presents the evolution pattern of GRF at different leg stiffnesses. From a comparison with the normalized GRF in Figure 26, it can be concluded that when parameter $\omega_{leg} = \sqrt{k_{leg}/m}$ is introduced, the two graphs exhibit nearly the same trend; that is, both produce a forward shift of the trough position in the shape of M and there exists a larger gap between the two peaks if ω_{leg} becomes larger.

With a request to investigate the effect of leg stiffness and damping on structural response and properties, we perform the analysis with fixed values for the following parameters: $\xi_{HR} = 0.5$, $\eta = 0.3$, and $m_{HR} = 75$ kg. The results of the numerical analysis are displayed in Figures 31–33. A two-staged characteristic is exhibited with the increased stiffness, which is the effect of leg damping on the acceleration response of the structure (Figure 31). When $k_{leg} < 17$ kN/m, a greater damping of the leg elicits more intense responses; when $k_{leg} > 17$ kN/m, the opposite is the case. Figure 32 illustrates that the greater the leg damping is, the more obvious the positive effect of stiffness on frequency increasing is; but when $k_{leg} = 15.96$ kN/m, the body mass shows a negative correlation with structural frequency. A similar feature is available in Figures 32 and 33, but the difference lies in that the effect of leg stiffness on structural damping is positively correlated at various damping values.

6.4. The Effects of Stiffness Ratio and Gait Frequency. Figures 34 and 35, respectively, present the effects of stiffness ratio on structure and GRF. As the stiffness ratio increases,

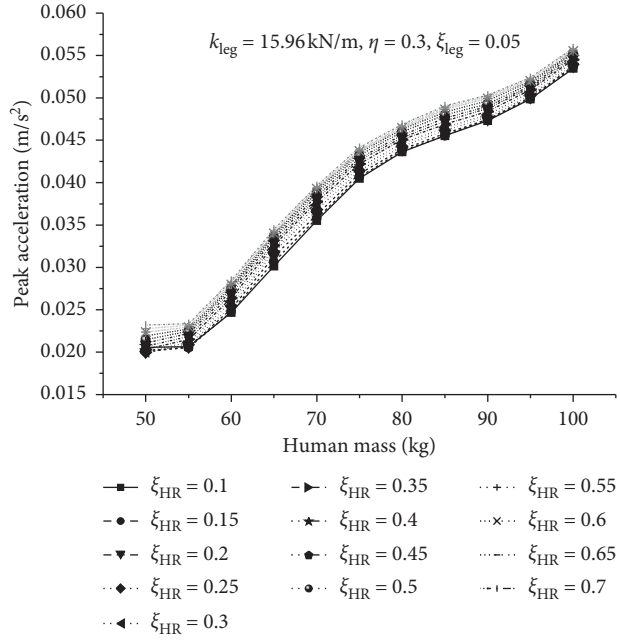

Figure 20: Peak acceleration under leg stiffness 15.96 kN/m, η = 0.3, and ξ_{leg} = 0.05.

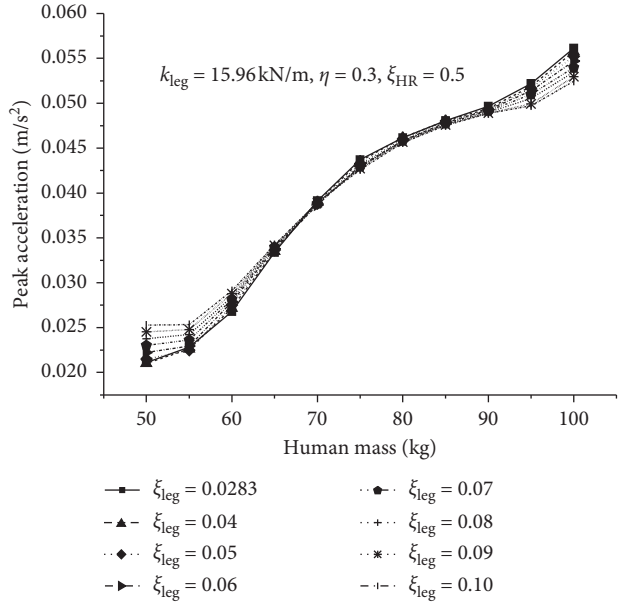

Figure 21: Peak acceleration under leg stiffness 15.96 kN/m, η = 0.3, and ξ_{HR} = 0.5.

the acceleration response of the structure indicates a downward tendency, while its frequency and damping ratio show a general uptrend with $\xi_{HR} = 0.5$, $\xi_{leg} = 0.05$, $m_{HR} = 75$ kg, and $k_{leg} = 18$ kN/m (Figure 34). As the stiffness ratio η increases, the GRF shape in Figure 35 exhibits "steeper" characteristics in both the ascending and descending phases. Compared to the GRF in Figures 26 and 30, Figure 35 features higher peaks and lower troughs, in which the shape shift also becomes less distinguishable.

Intended for identifying the relationship between GRF and pace frequency, we determine the relationship between step length and velocity as $L_s = 0.105\dot{x}_{HR} + 0.513$ according to Table 2, from which we derive the frequency of gait; that is, $f_s = (\dot{x}_{HR}/L_s)$. It is not hard to recognize that the shape and value of the GRF are particularly sensitive to gait frequency (Figure 36). As the gait frequency increases, the main features of changes of GRF can be summarized as follows：

(1) The duration of the single step will be shortened and the trough position will be moved forward.

(2) There are higher peaks, lower troughs, and a broader gap between the two values.

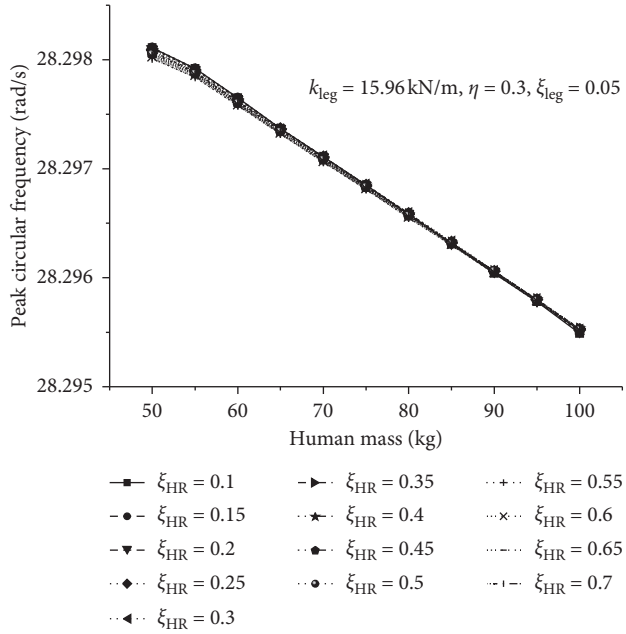

Figure 22: Peak frequency under leg stiffness 15.96 kN/m, η = 0.3, and ξ_{leg} = 0.05.

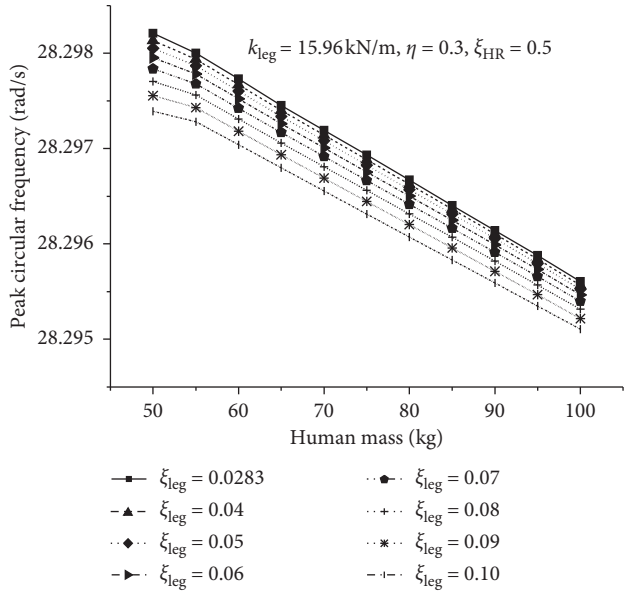

Figure 23: Peak frequency under leg stiffness 15.96 kN/m, η = 0.3, and ξ_{HR} = 0.5.

(3) Both the ascent and descent phases are "steeper."

(4) The difference in values between the two peaks is more distinguishable.

7. Discussion

In contrast to the classic bipedal walking models that treat the center of the body as a concentrated mass, the paper discusses the impact of the dynamics of other parts of the body on the bipedal walking model. We innovatively propose that other body parts can be equivalent to a continuum in which mass, stiffness, and damping distributions are included. The strategy of variable leg stiffness during the gait cycle helps introduce the concept of stiffness ratio. In order to guarantee the stability of the model, a self-determined mechanism is employed, where the velocity in the pedestrian movement process is assumed to be given in advance.

Numerical studies indicate that, under the same initial parameter conditions, a bipedal walking model that introduces the concept of the continuum can obtain a stable gait more efficiently than a classic model does. It simplifies the optimization process of initial parameters to achieve the stabilization of the gait compared to the model proposed by Gao et al. [29] and Qin et al. [27, 28]. In addition, a spectral

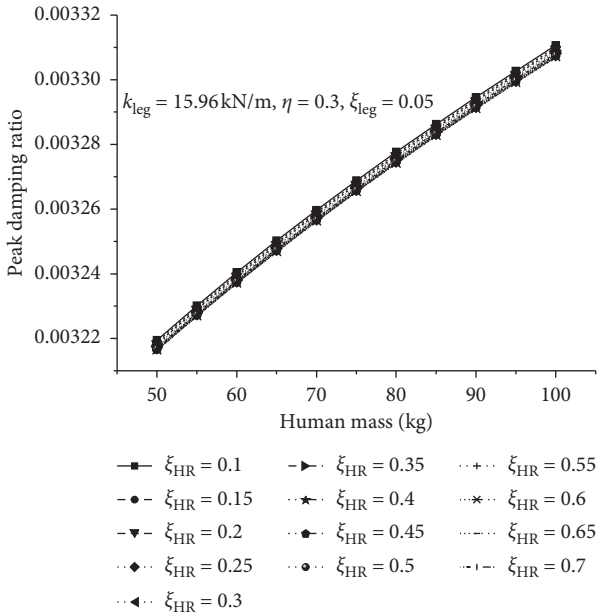

Figure 24: Peak damping ratio under leg stiffness 15.96 kN/m, η = 0.3, and ξ_{leg} = 0.05.

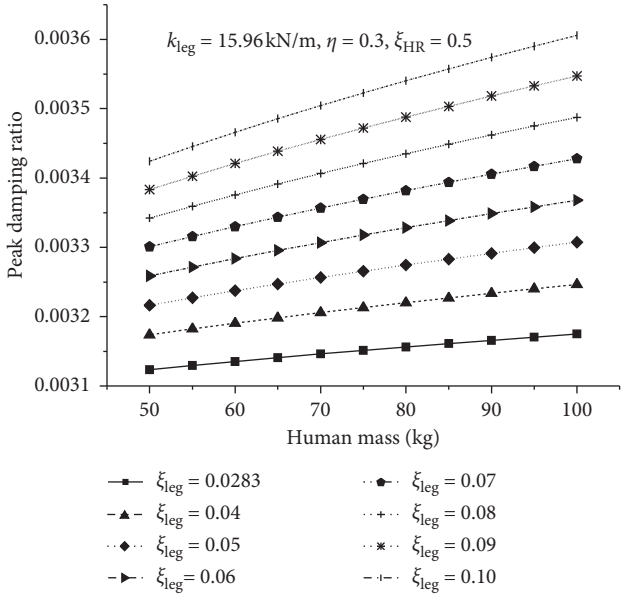

Figure 25: Peak damping ratio under leg stiffness 15.96 kN/m, η = 0.3, and ξ_{HR} = 0.5.

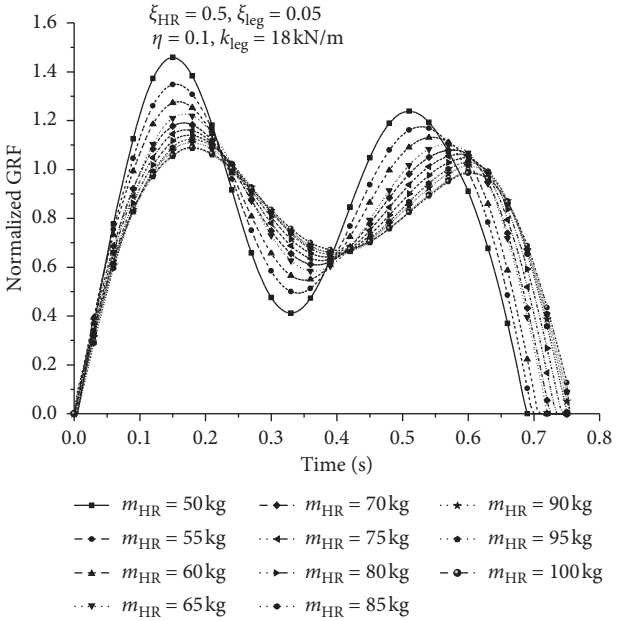

Figure 26: Normalized GRF under different human mass.

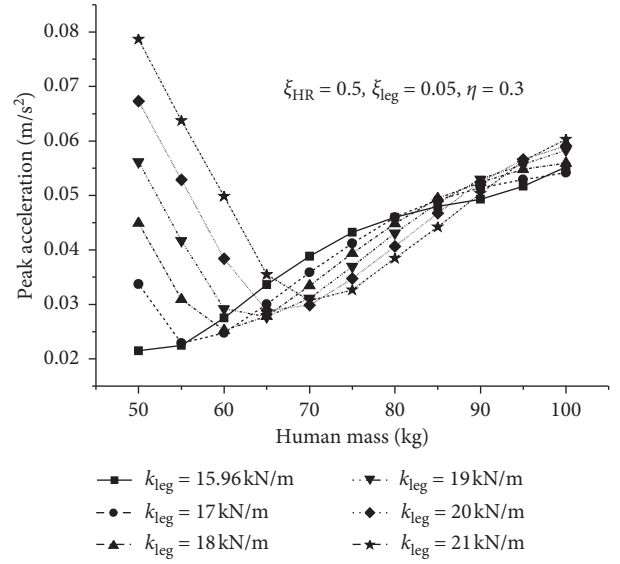

Figure 27: Peak acceleration under leg stiffness k_{leg} = 15.96 kN/m, η = 0.3, ξ_{HR} = 0.5, and ξ_{leg} = 0.05.

analysis of the acceleration response in the mid-span informs that the pedestrian load merits particular attention for it does produce multiplicative frequency effects in the evaluation of the human-induced response, especially when its frequency is close to the dominant frequency of the structure.

It is concluded from the numerical analysis that continuum damping has a negligible effect on the GRF and the damping of the structure. However, both continuum damping and leg damping exert a noticeable effect on the acceleration response of the structure, which suggests that the dynamic properties of the continuum are not negligible in human-structure interactions. The effect of continuum damping coupling with leg damping on the structure has not been reported. Compared to continuum damping, leg damping is more effective in reducing structural frequencies. In contrast to damping and leg stiffness, the influence of body mass on the structural response and associated dynamic properties is much more significant. The increasing body mass can provoke the structure's strong response, increase the damping ratio, reduce its frequency, and make GRF's double-peak feature more distinguishable. The effect

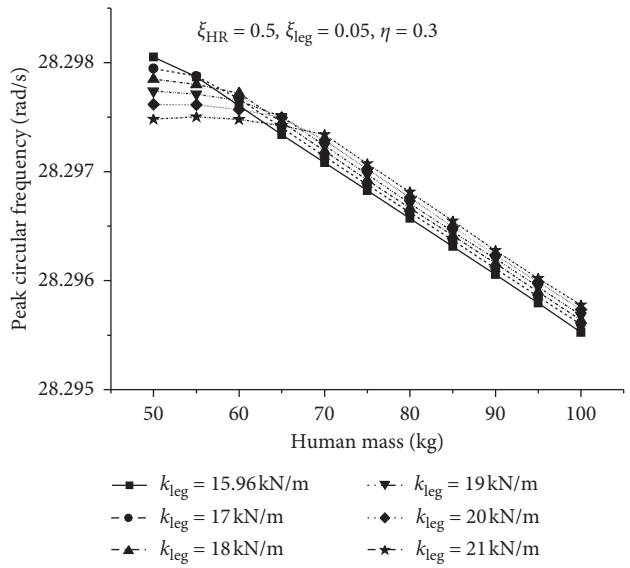

Figure 28: Peak frequency under leg stiffness k_{leg} = 15.96 kN/m, η = 0.3, ξ_{HR} = 0.5, and ξ_{leg} = 0.05.

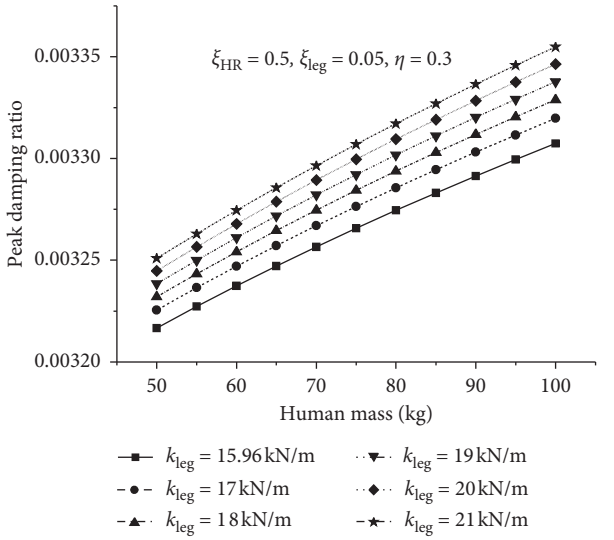

Figure 29: Peak damping ratio under leg stiffness k_{leg} = 15.96 kN/m, η = 0.3, ξ_{HR} = 0.5, and ξ_{leg} = 0.05.

of human leg stiffness on the acceleration response of the structure displays a much more complex pattern for it features a "U"-shaped tendency with increased body mass. The stiffness is positively correlated with the frequency of the structure if the body mass is large enough, but it is consistently correlated with the damping of the structure across a wide mass range. Leg stiffness is positively correlated with structural damping and frequency if body mass is a fixed constant. Meanwhile, it is revealed that both the stiffness

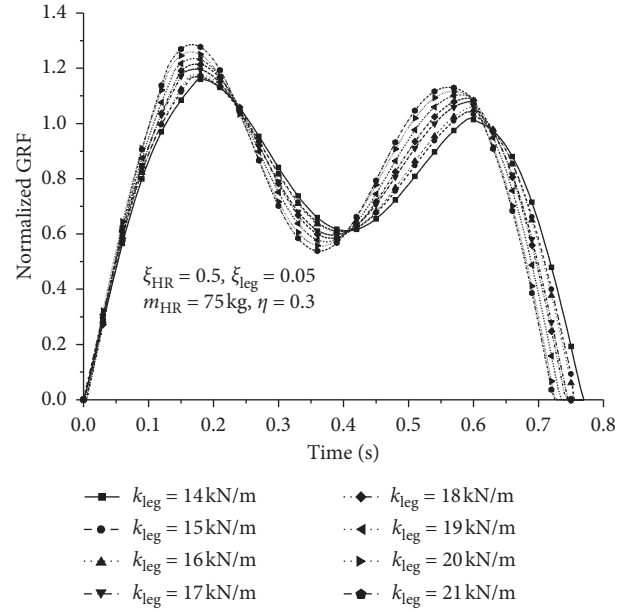

Figure 30: Normalized GRF under different leg stiffness.

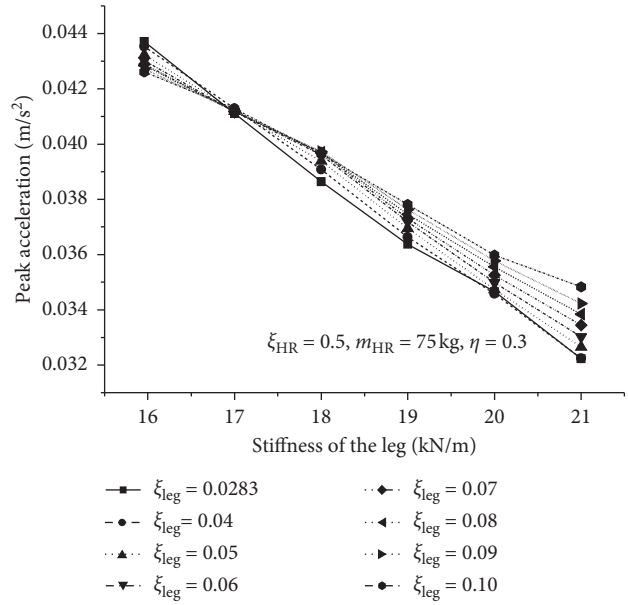

Figure 31: Peak acceleration under ξ_{HR} = 0.5, η = 0.3, and m_{HR} = 75.

ratio and the gait frequency have a significant effect on the GRF's shape.

If necessary, the bipedal model proposed in the paper that considers continuum dynamics can be utilized to evaluate the response and properties of pedestrian-structure interactions. The model takes the effects produced by the movement and

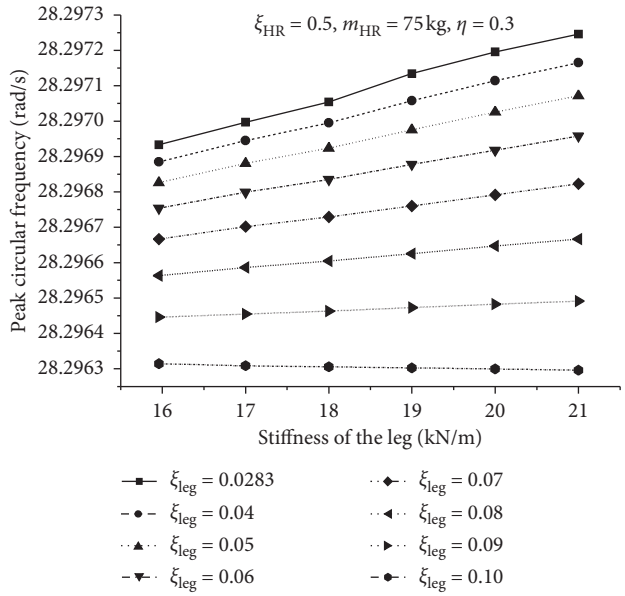

Figure 32: Peak frequency under $\xi_{HR} = 0.5$, $\eta = 0.3$, and $m_{HR} = 75$.

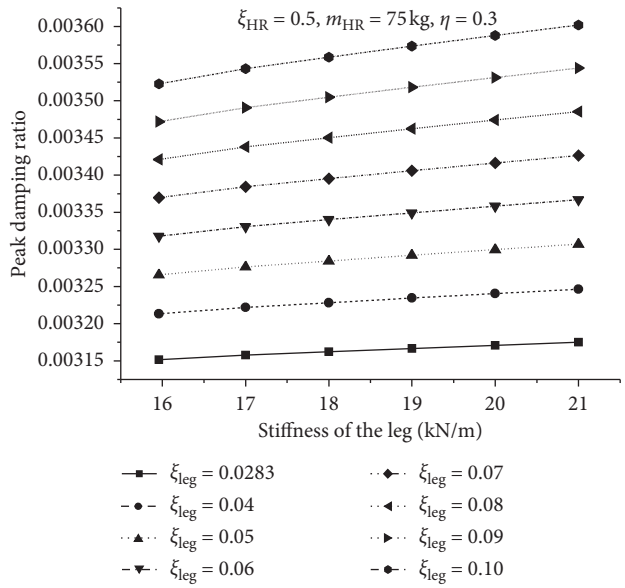

Figure 33: Peak damping ratio under $\xi_{HR} = 0.5$, $\eta = 0.3$, and $m_{HR} = 75$.

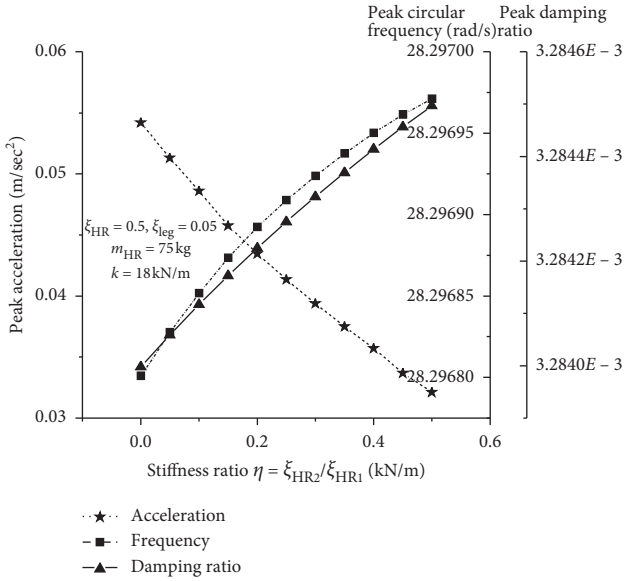

Figure 34: Peak acceleration, frequency, and damping ratio under $\xi_{HR} = 0.5$, $\xi_{leg} = 0.05$, $m_{HR} = 75$, and $k_{leg} = 18$ kN/m.

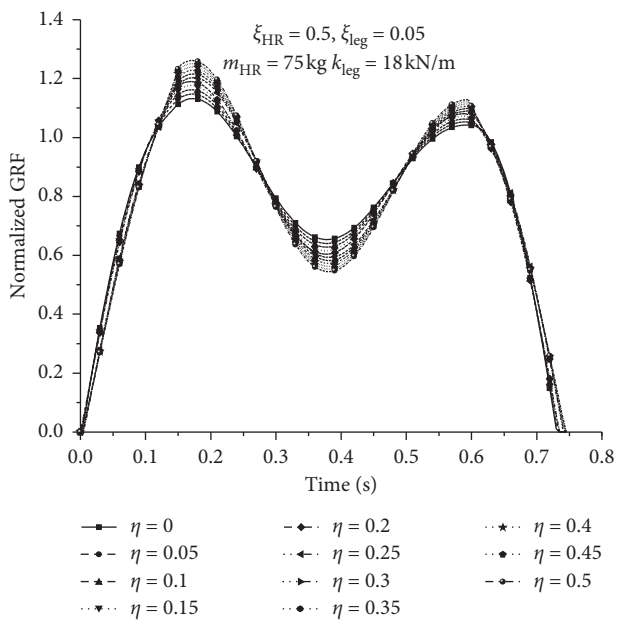

Figure 35: Normalized GRF under different stiffness ratio.

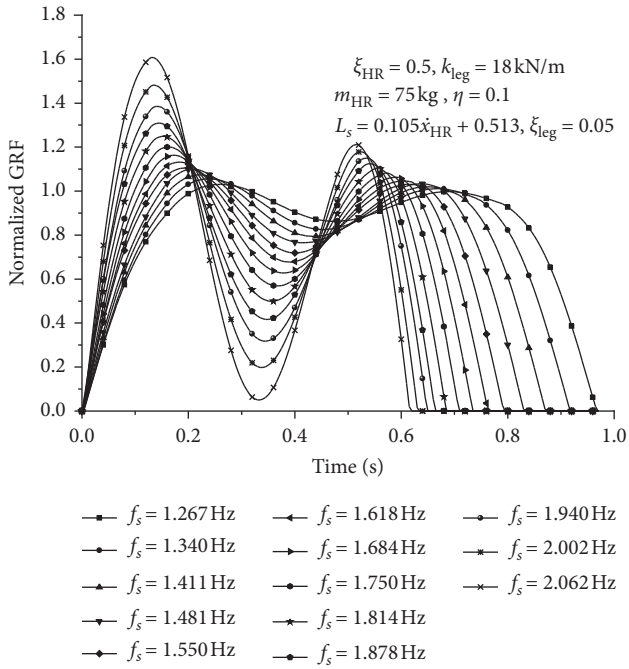

Figure 36: Normalized GRF under different gait frequencies.

dynamics of human walking into account and has a potential for a broader implementation in the design of long, soft-span structures. Meanwhile, the model involves the problem of individual variation in the crowd and can be applied to further study of crowd-structure systems.

Admittedly, the model has the following limitations.

(1) The model derivation in our paper is only applicable to Euler–Bernoulli beams and is limited in scope and application to other forms of structures

(2) The paper analyzes and evaluates the impact of walking pedestrians on the structure but does not cover the dynamic effects of other human actions such as jumping and running

8. Conclusion

In this paper, a human-structure interaction system with a pedestrian treated as a bipedal model and human mass treated as a continuum is derived using Lagrange equations to examine the influence of the continuum on the structural vertical response and its dynamics properties. A self-determined mechanism based on the assumption that the velocity is a given value is utilized to guarantee the stability of pedestrian-structure system when dynamic calculations are performed. Moreover, a novel stiffness strategy is employed to investigate different effects of stiffness strategy on the dynamic behaviour and GRF values based on the comparison with the classic strategy proposed by Qin et al. [27, 28].

Based on the mass distribution and stiffness strategy proposed by this paper, a numerical analysis is conducted. The results indicate that model parameters such as damping ratio of the continuum, leg stiffness, leg damping ratio, and mass of pedestrian have a significant influence on the dynamic properties of the pedestrian-structure system. The effect of these parameters on the shape and peak of the load curve of ground reaction forces is also conducted. The results have shown that the model including a continuum can achieve the stabilization of the gait and complete the calculation in a more efficient way, which is especially noticeable in structure with a short span. Moreover, the influence of the continuum damping on the response of the structure cannot be ignored. It is a rather interesting result, since most researchers are ignoring the distribution of the dynamic properties of the other parts of the body when the human-structure system is built. Pedestrian mass can significantly reduce the structure frequency, add structure damping, and modify the shape of the GRF and values of peaks. Other model parameters also have a nonnegligible contribution to structural behaviour. We note that the influences of model parameters on the structure are coupled to each other; for example, the overall impact of leg stiffness at various mass ranges on the structure's response exhibits different trends. The tendency of leg stiffness, pedestrian mass, and gait frequency on GRF displays a similar pattern.

The pedestrian-structure system that includes the continuum we propose has a potential for application in the design of long and flexible structures as well as the evaluation of human comfort induced by structure vibrations. The process of pedestrian-structure interaction can be obtained by setting appropriate parameters of the bipedal walking model, which opens a new field for further exploration on the design of long, flexible structures. Moreover, the model can be further extended to a 3D model to investigate the influence of pedestrian walking on the dynamics of structure in the lateral, forward, and vertical direction. The continuum can be further developed to a more complicated component based on the finite element method (FEM) to represent a more comprehensive condition of the mass and stiffness distribution of the human body.

Data Availability

The data supporting the findings of this study are included within the article.

Conflicts of Interest

The authors declare that there are no conflicts of interest regarding the publication of this paper.

Acknowledgments

The authors would like to thank HY L for language revision of this article. This study was supported by the National Natural Science Foundation of China (Grant No. 51278106) and the Project of Science and Technology Research and Development Program of China Railway Corporation (Grant No. P2018G049).

References

[1] S. Živanović, A. Pavic, and P. Reynolds, "Vibration serviceability of footbridges under human-induced excitation: a literature review," *Journal of Sound and Vibration*, vol. 279, no. 1-2, pp. 1–74, 2005.

[2] OHBDC, *Ontario Highway Bridge Design Code*, Highway Engineering Division, Ministry of Transportation and Commnication, Ontario, Canada, 1983.

[3] BS5400, *Concrete and Composite Bridges-Part 2: Specification for Loads*, British Standard Association, London, UK, 1978.

[4] International Organization for Standardization (ISO), "Bases for Design of Structures: Serviceability of Buildings and Walkways Against Vibrations," International Organization for Standardization (ISO), Geneva, Switzerland, 2007.

[5] EN 1995-2:2004, "Eurocode 5: design of timber structures—part 2: bridges," European Committee of Standardization, Brussels, Belgium, 2004.

[6] Technical Department for Transport, *Roads and Bridges Engineering, and Road Safety/French Association of Civil Engineering (SETRA/AFGC), Footbridges: Assessment of Vibrational Behaviour of Footbridges Under Pedestrian Loading*, SETRA/AFGC, Paris, France, 2006.

[7] M. Feldmann, Ch. Heinemeyer, M. Lukic et al., *Human-Induced Vibration of Steel Structures (Hivoss)*, Research Fund for Coal and Steel, European Commission, 2008.

[8] E. T. Ingólfsson, C. T. Georgakis, and J. Jönsson, "Pedestrian-induced lateral vibrations of footbridges: a literature review," *Engineering Structures*, vol. 45, pp. 21–52, 2012.

[9] V. Racic, A. Pavic, and J. Brownjohn, "Experimental identification and analytical modelling of human walking forces: literature review," *Journal of Sound and Vibration*, vol. 326, no. 1-2, pp. 1–49, 2009.

[10] F. Venuti and L. Bruno, "Crowd-structure interaction in lively footbridges under synchronous lateral excitation: a literature review," *Physics of Life Reviews*, vol. 6, no. 3, pp. 176–206, 2009.

[11] J. M. Biggs, *Introduction to Structural Dynamics*, McGraw-Hill College, New York, NY, USA, 1964.

[12] E. Agu and M. Kasperski, "Influence of the random dynamic parameters of the human body on the dynamic characteristics of the coupled system of structure-crowd," *Journal of Sound and Vibration*, vol. 330, no. 3, pp. 431–444, 2011.

[13] G. Busca, A. Cappellini, S. Manzoni, M. Tarabini, and M. Vanali, "Quantification of changes in modal parameters due to the presence of passive people on a slender structure," *Journal of Sound and Vibration*, vol. 333, no. 21, pp. 5641–5652, 2014.

[14] M. Kasperski, "Damping induced by pedestrians," in *Proceedings of the 9th International Conference on Structural Dynamics of EURODYN*, pp. 1059–1064, Porto, Portugal, July 2014.

[15] M. Willford, "Dynamic actions and reactions of pedestrians," in *Proceedings of the International Conference on the Design and Dynamic Behaviour of Footbridges*, pp. 66–73, Paris, France, November 2002.

[16] S. Živanović, A. Pavić, and E. T. Ingólfsson, "Modeling spatially unrestricted pedestrian traffic on footbridges," *Journal of Structural Engineering*, vol. 136, no. 10, pp. 1296–1308, 2010.

[17] P. Heinemann and M. Kasperski, "Damping induced by walking and running," *Procedia Engineering*, vol. 199, pp. 2826–2831, 2017.

[18] P. J. Archbold, *Interactive Load Models for Pedestrian Footbridges*, University College Dublin, Dublin, Ireland, 2004.

[19] C. C. Caprani, J. Keogh, P. Archbold, and P. Fanning, "Characteristic vertical response of a footbridge due to crowd loading," in *Proceedings of the 8th International Conference on Structural Dynamics of EURODYN*, pp. 978–985, Leuven, Belgium, 2011.

[20] S.-H. Kim, K.-I. Cho, M.-S. Choi, and J.-Y. Lim, "Development of human body model for the dynamic analysis of footbridges under pedestrian induced excitation," *Steel Structures*, vol. 8, no. 4, pp. 333–345, 2008.

[21] K. Van Nimmen, G. Lombaert, G. De Roeck, and P. Van den Broeck, "Human-induced vibrations of footbridges: the effect of vertical human-structure interaction," in *Proceedings of IMAC 34, the International Modal Analysis Conference*, Springer-Verlag, Orlando, FL, USA, January 2016.

[22] K. Van Nimmen, K. Maes, G. Lombaert, G. De Roeck, and P. Van den Broeck, "The impact of vertical human-structure interaction for footbridges," in *Proceedings of the 5th International Conference on Computational Methods in Structural Dynamics and Earthquake Engineering*, Crete Island, Greece, 2015.

[23] B. R. Whittington and D. G. Thelen, "A simple mass-spring model with roller feet can induce the ground reactions observed in human walking," *Journal of Biomechanical Engineering*, vol. 131, no. 1, Article ID 011013, 2009.

[24] S. Kim and S. Park, "Leg stiffness increases with speed to modulate gait frequency and propulsion energy," *Journal of Biomechanics*, vol. 44, no. 7, pp. 1253–1258, 2011.

[25] S. Kim and S. Park, "The oscillatory behavior of the CoM facilitates mechanical energy balance between push-off and heel strike," *Journal of Biomechanics*, vol. 45, no. 2, pp. 326–333, 2012.

[26] H. Lim and S. Park, "A bipedal compliant walking model generates periodic gait cycles with realistic swing dynamics," *Journal of Biomechanics*, vol. 91, pp. 79–84, 2019.

[27] J. W. Qin, S. S. Law, Q. S. Yang, and N. Yang, "Pedestrian-bridge dynamic interaction, including human participation," *Journal of Sound and Vibration*, vol. 332, no. 4, pp. 1107–1124, 2013.

[28] J. Qin, S. Law, Q. Yang, and N. Yang, "Finite element analysis of pedestrian-bridge dynamic interaction," *Journal of Applied Mechanics*, vol. 81, no. 4, pp. 1–15, 2014.

[29] Y.-A. Gao, Q.-S. Yang, and J.-W. Qin, "Bipedal crowd–structure interaction including social force effects," *International Journal of Structural Stability and Dynamics*, vol. 17, no. 7, Article ID 1750079, 2017.

[30] Y.-a. Gao and Q.-s. Yang, "A theoretical treatment of crowd–structure interaction," *International Journal of Structural Stability and Dynamics*, vol. 18, no. 1, Article ID 1871001, 2018.

[31] Q. Yang and Y. Gao, "A theory treatment of pedestrian-induced lateral vibration of structure," *Journal of Dynamic Systems, Measurement, and Control*, vol. 140, no. 6, Article ID 061004, 2018.

[32] T. WT, *Theory of Vibration and Applications*, Allan & Unwin, London, UK, 1966.

[33] J. N. Juang, *Applied System Identification*, Prentice Hall PTR, Upper Saddle River, NJ, USA, 1994.

[34] R. Sachse, "Modelling effects of human occupants on modal properties of slender structures," *Structural Engineer*, vol. 80, no. 5, pp. 21-22, 2002.

[35] T. Ji, D. Zhou, and Q. Zhang, "Models of a standing human body in vertical vibration," *Proceedings of the Institution of*

Civil Engineers - Structures and Buildings, vol. 166, no. 7, pp. 367–378, 2013.

[36] Q. Zhang, Y. Zhang, and T. Ji, "A continuous model of a standing human body in vertical vibration," *Engineering Review*, vol. 39, no. 2, pp. 132–140, 2019.

[37] H. Hong, S. Kim, C. Kim, S. Lee, and S. Park, "Spring-like gait mechanics observed during walking in both young and older adults," *Journal of Biomechanics*, vol. 46, no. 1, pp. 77–82, 2013.